

Causal Rule Ensemble: Interpretable Discovery and Inference of Heterogeneous Causal Effects

Falco J. Bargagli-Stoffi ^{*1}, Riccardo Cadei^{*1,2}, Kwonsang Lee ^{†3}, and Francesca Dominici¹

¹*Department of Biostatistics, Harvard T.H. Chan School of Public Health*

²*Department of Computer and Communication Science, EPFL*

³*Department of Statistics, Seoul National University*

Abstract

In health and social sciences, it is critically important to identify subgroups of the study population where a treatment has notable heterogeneity in the causal effects with respect to the average treatment effect. Data-driven discovery of heterogeneous treatment effects (HTE) via decision tree methods has been proposed for this task. Despite its high interpretability, the single-tree discovery of HTE tends to be highly unstable and to find an oversimplified representation of treatment heterogeneity. To accommodate these shortcomings, we propose Causal Rule Ensemble (CRE), a new method to discover heterogeneous subgroups through an ensemble-of-trees approach. CRE has the following features: 1) provides an interpretable representation of the HTE; 2) allows extensive exploration of complex heterogeneity patterns; and 3) guarantees high stability in the discovery. The discovered subgroups are defined in terms of interpretable decision rules, and we develop a general two-stage approach for subgroup-specific conditional causal effects estimation, providing theoretical guarantees. Via simulations, we show that the CRE method has a strong discovery ability and a competitive estimation performance when compared to state-of-the-art techniques. Finally, we apply CRE to discover subgroups most vulnerable to the effects of exposure to air pollution on mortality for 35.3 million Medicare beneficiaries across the contiguous U.S.

Keywords: Causal Inference, Machine Learning, Heterogeneous Treatment Effects, Interpretability, Sensitivity Analysis, Air Pollution Epidemiology

We are grateful for helpful feedback from organizers and participants at Harvard University, George Washington University, Sungkyunkwan University, St. Gallen University, KU Leuven, IMT School for Advanced Studies seminars, at the Online Causal Inference seminar (OCIS), at the IMS International Conference on Statistics and Data Science (ICSDS), at the Health Econometrics Workshop at Emory University, at the Data Science for Impact Evaluation Webinar (DSIE), and the European Causal Inference Meeting (EUROCIM). This work was supported by EPA grant (83587201-0), NIH grants (R01ES026217, R01MD012769, R01ES028033, 1R01AG060232-01A1, 1R01ES030616, 1R01AG066793-01R01, 1R01ES029950) as well as the Alfred P. Sloan Foundation Grant for the development of “Causal Inference with Complex Treatment Regimes: Design, Identification, Estimation, and Heterogeneity”, the VPR - Harvard University grant on “Climate Change Solutions Fund” and the Harvard Data Science Initiative Postdoctoral Research Fund Award.

*Co-first authors.

†Corresponding author. kwonsanglee@snu.ac.kr

1 Introduction

1.1 Motivating Application

The U.S. Environmental Protection Agency (EPA) has recently set the goal to achieve environmental justice by addressing the disproportionate vulnerabilities in adverse human health effects due to exposure to air pollution (U.S. Environmental Protection Agency; 2022b). According to the EPA, environmental justice is defined as “*no group of people should bear a disproportionate burden of environmental harms and risks*” (see U.S. Environmental Protection Agency; 2022a, page 116). In the effort to promote environmental justice, the EPA has called for scientific studies that would inform the understanding of disproportionate health impacts of air pollution, with particular attention on demographic-specific information (U.S. Environmental Protection Agency; 2022a). Despite strong evidence that exposure to air pollution increases the risk of mortality and morbidity (see, e.g., Schwartz et al.; 2021; Wu, Braun, Schwartz, Kioumourtoglou and Dominici; 2020; Nethery et al.; 2020; Carone et al.; 2020), little is known about which are the subgroups—i.e., subsets of the population characterized by a given covariate-profile (e.g., female individuals, low-income & male individuals)—who are most vulnerable or resilient to exposure to higher levels of air pollution.

Previous air pollution vulnerability studies are few and limited in their scope. Lee et al. (2021) and Zorzetto et al. (2023) recently proposed to causally assess exposure heterogeneity in air pollution via machine learning and Bayesian non-parametric methodologies, respectively. However, these studies are limited by the scalability of the employed methods, and their coverage is restricted to selected areas of the United States—i.e., New England and California. Di et al. (2017) estimated associations between long-term exposure to air pollution and mortality rates for pre-specified population subgroups defined by age, gender, and race categories. Despite its national coverage, this study has the main limitations of not directly answering a causal question, but an associational one and providing a very limited heterogeneity exploration—i.e., heterogeneous associations are estimated just for a predefined and very limited set of characteristics (e.g., sex, age, race). Thus, in spite of the urgency of a nationwide study that would extensively explore the heterogeneous health effects of air pollution, a national study on this topic is not yet available.

Furthermore, most analyses on the effects of fine particulate matter ($\text{PM}_{2.5}$) on human health are conducted at the ZIP code or at the county level. Nevertheless, such analyses may mask important individual-level sources of heterogeneity and, most importantly, might expose the results to ecological fallacy (Freedman; 1999). The ecological fallacy, also known as the ecological inference fallacy or population fallacy, refers to the incorrect interpretation of results of statistical analyses, where conclusions about individuals are drawn from inferences made about the group to which they belong. Such fallacies in air pollution epidemiology studies have been recently acknowledged (see, e.g., Wu, Netherly, Sabath, Braun and Dominici; 2020). To our knowledge, no study has yet considered the heterogeneous causal effects of exposure to air pollution at an *individual level*.

To goal of our motivating application is to accommodate for this shortcoming and answer the EPA call by providing nationwide data-driven evidence regarding the most vulnerable subgroups to exposure to air pollution via an individual-level analysis. In particular, we aim to develop new methods in causal inference and machine learning with the goal of identifying de novo which subgroups of the Medicare population are most vulnerable or resilient to long-term exposure to $\text{PM}_{2.5}$ on mortality.

To do so, we acquired and integrated the data on 35,331,290 Medicare beneficiaries (i.e., individuals 65 years of age or older) across the entire United States for the period 2010-2016. We consider a binary exposure, indicating whether each individual has been exposed to $\text{PM}_{2.5}$ greater than $12 \mu\text{g}/\text{m}^3$ or not. This exposure is the current National Ambient Air Quality Standard (NAAQS) set by the EPA. We link exposure to two-year annual $\text{PM}_{2.5}$ during 2010-2011 at the zip code level to mortality during the 5-years period 2012-2016 and several potential confounders, both at the individual, zip-code, and county level. Our study focuses on exploring the heterogeneity in the causal effects within the four U.S. census geographic regions—namely, Northeast, Midwest, West, and South—that are often utilized in investigations related to the impact of air pollution exposure. More details about the study design and results are illustrated in section 5.

1.2 Contribution and Related Works

The bulk of heterogeneous treatment effect (HTE) literature focuses on two major tasks (Dwivedi et al.; 2020): (i) estimating HTEs by examining the conditional average treatment effect (CATE); (ii) discovering subgroups of a population characterized by HTE.

Seminal works on estimating the CATE rely on nearest-neighbor matching and kernel methods (Crump et al.; 2008; Lee; 2009). Other non-parametric machine learning methods such as the random forest (Breiman; 2001) and Bayesian additive regression tree (BART) (Chipman et al.; 2010) have been extended to estimate heterogeneity in causal effects—see, e.g., Foster et al. (2011), Hill (2011) and Hahn et al. (2020). Wager and Athey (2018) and Athey et al. (2019) developed forest-based methods for the estimation of HTEs. They also provide an asymptotic theory for the conditional treatment effect estimators and valid statistical inference. Recently, two-stage doubly robust CATE estimators have been proposed first to generate doubly-robust pseudo outcomes and then regress them onto an a priori defined set of effect modifiers (Kennedy; 2020; Semenova and Chernozhukov; 2021).

Various methodologies have also been proposed to identify subgroups characterizing the heterogeneity in treatment effects (Imai et al.; 2013; Qian and Murphy; 2011; Kennedy et al.; 2017; Nie and Wager; 2017). Some methods first estimate the CATE as a function of some set of covariates and then identify heterogeneous subgroups in a second stage (Foster et al.; 2011; Bargagli-Stoffi et al.; 2020; Hahn et al.; 2020; Bargagli-Stoffi, De Witte and Gnecco; 2022). Another approach is the direct data-driven discovery of heterogeneous subgroups (Wang and Rudin; 2022; Nagpal et al.; 2020). Many of the methodologies in this category are decision tree-based methodologies (see, e.g., Athey and Imbens; 2016; Bargagli-Stoffi and Gnecco; 2020; Lee et al.; 2021; Yang et al.; 2021; Bargagli-Stoffi et al.; 2020; Bargagli-Stoffi, De Witte and Gnecco; 2022). Tree-based approaches have been widely adopted for treatment effect heterogeneity due to their appealing features. In fact, these methods are based on efficient and easily implementable recursive mathematical programming (e.g., maximization in the heterogeneous treatment effects), they can be easily tweaked and adapted to different scenarios on the basis of the research question of interest, and they guarantee a high degree of interpretability.

Despite their appealing features, single-tree heterogeneity discovery is characterized by two main limitations: (i) instability in the identification of the subgroup, and (ii) reduced exploration of the potential heterogeneity. Firstly, single-tree-based subgroup identification is sensitive to variations in the training sample—e.g., if the data are slightly altered, a completely different set of discovered subgroups might be found (namely, the model variance is high) (Breiman; 1996; Hastie et al.; 2009; Kuhn et al.; 2013). Secondly, it may fail to explore a vast number of potential subgroups (limited subgroup exploration)—e.g., the subgroups discovered are just the ones that can be represented by a single tree (Kuhn et al.; 2013; Spanbauer and Sparapani; 2021). To illustrate, consider a scenario in which two distinct factors are independently contributing to the heterogeneity in treatment effects. In such cases, a single tree algorithm may detect only one of these factors, failing to identify the second. In instances where both factors are identified, they are detected sub-optimally as an interaction between the two variables rather than as distinct drivers of the treatment heterogeneity.

To account for these shortcomings, we propose a novel Causal Rule Ensemble (CRE) method that uses multiple trees rather than a single tree to uncover, in a data-driven way, heterogeneity patterns in the treatment effect via decision rules. CRE provides (i) an interpretable representation of the HTE, (ii) via an extensive exploration of complex heterogeneity patterns, while (iii) guaranteeing high stability in the discovery. We also develop a general two-stage estimation approach for the conditional causal effects of the discovered subgroups and provide theoretical guarantees.

CRE ensures interpretability providing a linear decomposition of the HTE in terms of *decision rules*. Interpretability is a non-mathematical concept, yet it is often defined as the degree to which a human can understand the cause of a decision (Kim et al.; 2016; Miller; 2019; Lakkaraju et al.; 2016; Wang and Rudin; 2022). *If-then* decision rules are highly interpretable as they resemble human decision-making processes. The discovery of these decision rules is obtained via an extensive exploration of complex heterogeneity patterns. In particular, CRE generates candidate decision rules from an ensemble of decision trees extracting heterogeneity in the treatment effect. Among these candidate decision rules, CRE proposes to extract only a stable set of decision rules characterizing the HTE by a rework of the stability selection algorithm (Meinshausen and Bühlmann; 2010). The stability of statistical results relative to “reasonable” perturbations to data and to the model

used is critically important for reproducible research (Yu; 2013). Next to enhanced reproducibility, the stability selection algorithm allows also control for finite sample false discovery error.

Finally, CRE provides a two-stage estimation approach for the estimation of the coefficients in the discovered linear model of the conditional average treatment effect. In the first stage, pseudo-outcomes are produced using any of the available techniques for the estimation of HTE at the individual level. In the second stage, these pseudo-outcomes are regressed onto the discovered rules. Different subsamples are used for rules discovery and estimation in the prevention of overfitting (i.e., honest splitting Athey and Imbens (2016)). We provide theoretical results that guarantee the consistency and asymptotic normality of the estimated model coefficients. We also note that the proposed two-stage estimation is similar in spirit (even if the target estimands are different) to the Double Robust (DR) learner proposed by Kennedy (2020).

The remainder of the paper is organized as follows. In section 2, we introduce the potential output framework and interpretable heterogeneous treatment effect discovery via decision rules. In section 3, we introduce the proposed CRE methodology. In section 4, we validate this methodology by simulated experiments, which are further extended in the Supplementary Material. In section 5, we propose to answer to EPA’s call for environmental justice, applying the CRE method to assess vulnerability and resilience from air pollution exposure in the United States. section 6 discusses the strengths and weaknesses of our proposed approach and areas of future research. CRE is implemented in an R package available on CRAN. Full documentation for the package can be found at <https://nsaph-software.github.io/CRE/>.

2 Problem Formulation

2.1 Potential Outcomes Framework

Let \mathcal{I} be a sample of N individuals. For an individual i , with $i = 1, \dots, N$, let $\mathbf{X}_i \in \mathcal{X} \subseteq \mathbb{R}^P$ be the set of covariates characterizing i , $Z_i \in \{0, 1\}$ be i ’s observed (binary) treatment, and $Y_i \in \mathcal{Y} \subseteq \mathbb{R}$ be i ’s observed outcome. Following the potential outcome framework (Rubin; 1974), for each individual, $i \in \mathcal{I}$, we define $Y_i(1)$ and $Y_i(0)$ as the potential outcomes under treatment and control,

respectively; and the Individual Treatment Effect (ITE): $\tau_i := Y_i(1) - Y_i(0)$. The Average Treatment Effect is the expected value of the ITE: $\bar{\tau} := \mathbb{E}[Y_i(1) - Y_i(0)]$. The Conditional Average Treatment Effects (CATE) on \mathbf{x} is the expected value of the ITE conditioning over a set of covariates \mathbf{x} :

$$\tau(\mathbf{x}) := \mathbb{E}[Y_i(1) - Y_i(0) | \mathbf{X}_i = \mathbf{x}]. \quad (2.1)$$

The CATE can be specified at different levels of *granularity*. For instance, at the highest level of granularity, one might want to estimate the ITE. At a lower level of granularity, one might want to estimate the average treatment effect for some *subgroups* of the population. This latter estimand can also be referred to as the Group Average Treatment Effect (GATE) (Jacob; 2019). Both the ITE and GATE are special cases of CATE. Throughout this paper, we will simply use the CATE rather than the GATE when referring to the estimated effects in the subgroups detected by the proposed algorithm.

Since only one potential outcome can be observed for each individual—the fundamental problem of causal inference (Holland; 1986)—we need to rely on a few assumptions to identify the causal estimands of interest.

Assumption 1 (Stable Unit Treatment Value Assumption (SUTVA)).

- (i). $Y_i(Z_i) = Y_i, \quad \forall i \in \mathcal{I}$
- (ii). $Y_i(Z_i) = Y_i(Z_1, Z_2, \dots, Z_i, \dots, Z_N) \quad \forall i \in \mathcal{I}.$

SUTVA enforces that for each individual i , i 's outcome is simply a function of i 's treatment. This is a combination of (i) consistency (no different versions of the treatment levels assigned to each unit) and (ii) no interference assumption (among the individuals) (Rubin; 1986).

Assumption 2 (Overlap).

$$0 < e(\mathbf{x}) < 1 \quad \forall \mathbf{x} \in \mathcal{X},$$

where $e(\mathbf{x}) = \mathbb{E}[Z_i = 1 | \mathbf{X}_i = \mathbf{x}]$ is the propensity score (Rosenbaum and Rubin; 1983).

The overlap assumption states that, for each unit, the probability of receiving either treatment is

bounded away from zero and one.

Assumption 3 (Unconfoundedness).

$$(Y_i(1), Y_i(0)) \perp\!\!\!\perp Z_i \mid \mathbf{X}_i, \quad \forall i \in \mathcal{I}.$$

The unconfoundedness assumption states that, for each unit i , the two potential outcomes depend on \mathbf{X}_i , but are independent of Z_i conditioning on \mathbf{X}_i .

Under Assumptions 1, 2 and 3, the CATE can be identified as:

$$\tau(\mathbf{x}) = \mathbb{E}[Y_i \mid \mathbf{X}_i = \mathbf{x}, Z_i = 1] - \mathbb{E}[Y_i \mid \mathbf{X}_i = \mathbf{x}, Z_i = 0]. \quad (2.2)$$

2.2 Interpretable Heterogeneity Discovery

Several algorithms have already been proposed for CATE estimation under the above-mentioned assumptions (see, e.g., [Hill; 2011](#); [Foster et al.; 2011](#); [Wager and Athey; 2018](#); [Hahn et al.; 2020](#); [Athey et al.; 2019](#)). Although they can estimate the ITE accurately, these algorithms don't provide an interpretable characterization of the CATE. To account for this shortcoming, we provide a new CATE characterization—in terms of decision rules—that is highly interpretable.

2.3 Decision Rules

A decision rule r is a general function on the covariates' space \mathcal{X} characterizing a specific subgroup $S \subseteq \mathcal{X}$. We particularly focus on (interpretable) decision rules whose support (i.e., characterized subgroup) decompose as $S = S_1 \times \cdots \times S_P$ where $S_p \subseteq \mathbb{R}$ for all $p \in \{1, \dots, P\}$. A decision rule is a mapping from the covariates space to $\{0,1\}$: $r: \mathcal{X} \rightarrow \{0,1\}$. In the rest of the paper, we use *decision rule* referring to the specific definition:

$$\mathbf{x} \mapsto r(\mathbf{x}) := \prod_{p=1}^P \mathbf{1}(x_p \in S_p) \quad (2.3)$$

In Figure 1, we report a dummy (binary) decision tree to provide a few examples of decision rules with two binary covariates x_F (for female) and x_Y (for young). Indeed, each node in a

decision tree (with the exclusion of the root), combining the conditions of all its ancestors, agrees with the above definition of decision rule. For instance, the young female subgroup is expressed by $r_4(\mathbf{x}) = \mathbb{1}(x_F = 1) \cdot \mathbb{1}(x_Y = 1)$; and the male subgroup is expressed by $r_1(\mathbf{x}) = \mathbb{1}(x_F = 0)$, where the second term in the product is removed since equal to 1.

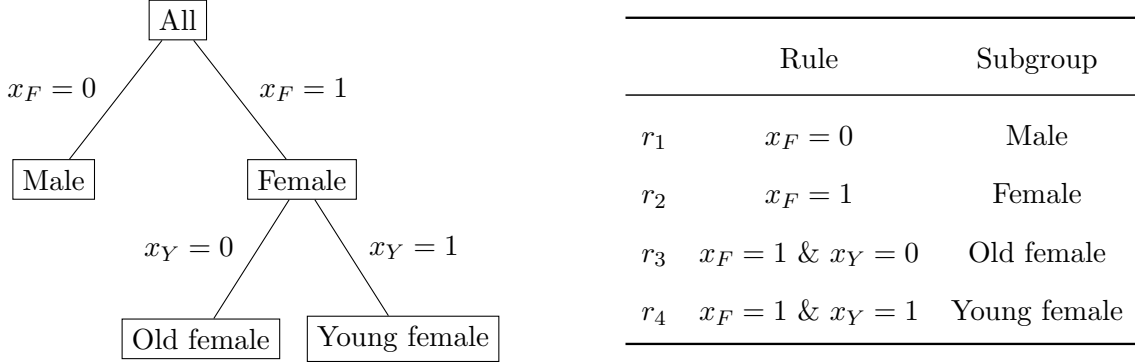


Figure 1: An example decision tree (left) and the corresponding decision rules (right). Note that, in the Causal Rule Ensemble algorithm, for each decision tree, we consider only the decision rules corresponding to the terminal nodes, in this example r_1, r_3 and r_4 .

2.4 Treatment Effect Linear Decomposition

We enforce interpretability in heterogeneous treatment effect estimation relying on the following assumption:

Assumption 4 (Treatment Effect Linear Decomposition). *Let $\mathcal{R} = \{r_m\}_{m=1}^M$ a set of decision rules. For each individual $i \in \mathcal{I}$, the (individual) treatment effect can be linearly decomposed as follows:*

$$\tau_i = \bar{\tau} + \sum_{m=1}^M \alpha_m(\mathcal{R}) \cdot r_m(\mathbf{X}_i) + \nu_i \quad (2.4)$$

where ν_i is an unobserved and independent additive noise—with $\mathbb{E}[\nu] = 0$ and $\text{Var}[\nu] = \sigma^2$ —and $\alpha_m(\mathcal{R})$ are the model coefficients.

Assumption 4 states that the (individual) treatment effect can be decomposed in (i) average effect (ATE), (ii) additive contributions $\alpha_m(\mathcal{R})$ for all the activated rules (we say that a decision rule is activated if evaluated on its support) characterizing the heterogeneity, and (iii) noise (ν_i).

In terms of the conditional expectation, Equation 2.4 becomes:

$$\tau(\mathbf{x}) = \bar{\tau} + \sum_{m=1}^M \alpha_m(\mathcal{R}) \cdot r_m(\mathbf{x}) \quad (2.5)$$

and it represents a step-wise approximation of the Conditional Average Treatment Effect $\tau(\mathbf{x})$ (which holds perfectly if the covariate space is finite). Please note that similar decompositions of the CATE have been proposed in the literature ([Kennedy; 2020](#); [Semenova and Chernozhukov; 2021](#), see, e.g.,).

For each rule r_m , the coefficient $\alpha_m(\mathcal{R})$ represents the additive contribution to the CATE, fixing the values of all the other decision rules. In formula:

$$\begin{aligned} \alpha_m(\mathcal{R}) := & \mathbb{E}[Y_i(1) - Y_i(0) | r_1(X_i) = \rho_1, \dots, r_m(X_i) = 1, \dots, r_M(X_i) = \rho_M] \\ & - \mathbb{E}[Y_i(1) - Y_i(0) | r_1(X_i) = \rho_1, \dots, r_m(X_i) = 0, \dots, r_M(X_i) = \rho_M] \end{aligned} \quad (2.6)$$

where $\rho_1, \dots, \rho_{m-1}, \rho_{m+1}, \dots, \rho_M \in \{0, 1\}$. In particular, $\alpha_m(\mathcal{R})$ represents the additive contribution to the ATE, when all the other rules are set to 0:

$$\alpha_m(\mathcal{R}) := \mathbb{E}_i \left[Y_i(1) - Y_i(0) | X_i \in \left\{ \mathbf{x} \in \mathcal{X} : \left[r_m(\mathbf{x}) \cdot \prod_{\substack{k=1 \\ k \neq m}}^M (1 - r_k(\mathbf{x})) \right] = 1 \right\} \right] - \bar{\tau} \quad (2.7)$$

In the context of the toy example in Figure 1, we can imagine $\alpha_m(\mathcal{R})$ being the additive effect when just one of the four rules is activated and the other are not.

In the rest of the paper, we refer to the coefficient $\alpha_m(\mathcal{R})$ as the Additive Average Treatment Effect (AATE) of the m -th rule, and for simplicity of language, we remove its dependency on \mathcal{R} .

Assumption 4, can be rewritten in a matrix form as:

$$\boldsymbol{\tau} = \bar{\tau} + R\boldsymbol{\alpha} + \boldsymbol{\nu} \quad (2.8)$$

where $\boldsymbol{\tau} \in \mathbb{R}^N$ is the vector of (unobserved) Individual Treatment Effects, $\bar{\tau} \in \mathbb{R}$ is the Average Treatment Effect, $\boldsymbol{\alpha} \in \mathbb{R}^M$ is the vector of AATEs, $\boldsymbol{\nu} \in \mathbb{R}^N$ is a vector of heteroscedastic and

independent additive noise and $R \in \{0, 1\}^{N \times M}$ is a matrix of $N \times M$ decision rules. Each element $R_{i,j} = r_j(X_i)$ for all $i \in \{1, \dots, N\}$ and $j \in \{1, \dots, M\}$, and for example:

$$R = \begin{matrix} & r_1(\cdot) & r_2(\cdot) & \dots & r_M(\cdot) \\ \mathbf{X}_1 & \left(\begin{array}{cccc} 0 & 1 & \dots & 0 \\ 0 & 0 & \dots & 1 \\ \vdots & \vdots & \ddots & \vdots \\ 1 & 0 & \dots & 0 \end{array} \right) \\ \mathbf{X}_2 & & & & \\ \vdots & & & & \\ \mathbf{X}_N & & & & \end{matrix}.$$

In this framework, interpretable heterogeneous discovery corresponds to finding a stable and minimal set of decision rules \mathcal{R} satisfying Equation 2.4, and HTE inference corresponds to estimation and inference on the α (AATEs) parameters.

3 Causal Rule Ensemble

In this section, we introduce Causal Rule Ensemble (CRE), a new algorithm for interpretable inference of heterogeneous causal effects through the linear treatment effect decomposition by decision rules introduced in the previous section.

Assuming the setup described in Section 2.1, we first divide the observational dataset into two subsamples: a discovery subsample (\mathcal{I}^{dis}) and an inference subsample (\mathcal{I}^{inf}). In the discovery step, we use \mathcal{I}^{dis} to select the set of decision rules $\hat{\mathcal{R}}$ robustly describing the heterogeneity in the treatment effect. In the estimation step, we use \mathcal{I}^{inf} to estimate the corresponding linear CATE decomposition in terms of decision rules. The idea of sample splitting is not new in statistics, and the earliest references can be traced back to [Stone \(1974\)](#) and [Cox \(1975\)](#). It is now commonly used also in the HTE literature to prevent overfitting and it is referred to as *honest splitting* ([Athey and Imbens; 2016](#); [Lee et al.; 2021](#)).

The following schematic summary illustrates the main steps of the proposed methodology. In the rest of the section, we discuss in detail all the steps of the proposed procedure and its theoretical guarantees.

Algorithm Causal Rule Ensemble (CRE)

Inputs: covariates matrix X , (binary) treatment vector \mathbf{z} , and observed response vector \mathbf{y} .

Outputs: (i) a set of interpretable decision rules $\hat{\mathcal{R}} = \{\hat{r}_m\}_{m=1}^M$,
(ii) ATE $\hat{\tau}$ and AATEs $\hat{\alpha}$ estimates and confidence intervals,

Procedure:

$(X^{dis}, \mathbf{z}^{dis}, \mathbf{y}^{dis}), (X^{inf}, \mathbf{z}^{inf}, \mathbf{y}^{inf}) \leftarrow \text{HonestSplitting}(X, \mathbf{z}, \mathbf{y})$

i. Discovery

$\hat{\tau}^{dis} \leftarrow \text{EstimateITE}(X^{dis}, \mathbf{z}^{dis}, \mathbf{y}^{dis})$ \triangleright e.g. AIPW, CF, BCF, BART, S/T/X-Learner (Section 3.1.1)
 $\hat{\mathcal{R}}' \leftarrow \text{GenerateRules}(X^{dis}, \hat{\tau}^{dis})$ \triangleright i.e., tree-ensemble method (Section 3.1.2)
 $\hat{\mathcal{R}} \leftarrow \text{RulesSelection}(\hat{\mathcal{R}}', X^{dis}, \hat{\tau}^{dis})$ \triangleright Stability Selection (Section 3.1.3)

ii. Inference

$\hat{\tau}^{inf} \leftarrow \text{EstimateITE}(X^{inf}, \mathbf{z}^{inf}, \mathbf{y}^{inf})$ \triangleright e.g. AIPW, CF, BCF, BART, S/T/X-Learner (Section 3.2.1)
 $\hat{\alpha} \leftarrow \text{EstimateAATE}(\hat{\mathcal{R}}, X^{inf}, \hat{\tau}^{inf})$ \triangleright Linear Decomposition (Section 3.2.2)

3.1 Discovery

Discovery is the first step of the Causal Rule Ensemble. It is itself divided into three steps, with the goal of discovering a stable set of decision rules approximating the Conditional Average Treatment Effect via Equation 2.8. First, the Individual Treatment Effect (pseudo-outcomes) is estimated by any causal-machine learning methodology (see Supplementary material for a brief overview of some of the possible methods). Second, an ensemble of trees algorithm (e.g., random forest) is trained to discover the heterogeneity in the estimated treatment effects (*fit-the-fit*), and a set of candidate decision rules is extracted. Finally, only a robust subset of the proposed decision rules is selected based on the stability selection algorithm.

3.1.1 Individual Treatment Effect Estimation

For each individual $i \in \mathcal{I}^{dis}$, we estimate the corresponding Individual Treatment Effect $\hat{\tau}_i^{dis}$, relying on Assumption (1)-(3). Causal Rule Ensemble is model-agnostic with respect to the used ITE estimators, and any algorithm can be used, leading to different convergence properties. For a brief overview of the six ITE estimators compared in the simulations, see the Supplementary Material.

3.1.2 Rules Generation

We detect the heterogeneity in the treatment effect by a *fit-the-fit* approach. Once the Individual Treatment Effect estimates on the discovery sample are obtained, we fit these estimates ($\hat{\tau}_i^{dis}$) from the observed covariates (\hat{X}_i^{dis}) by a tree-ensemble method (i.e., Random Forest (Breiman; 2001), Gradient Boosting Machine (Friedman; 2001)).

Several variants of tree-ensemble methods can be considered, for example modifying the splitting criteria in the forest generation to enforce heterogeneity discovery. Once the forest is generated, we test, a posteriori, the predictive performance of each terminal node, comparing an error metric for the model with and without that leaf. If the performances drop less than a certain threshold (t_{decay}), the node is discarded (pruned) as not significant for prediction (Deng; 2019).

We associate each leaf (terminal node) in the resulting forest with the corresponding decision rule obtained by combining the conditions of all its ancestors. Then, we collect all the distinct decision rules associated with the leaves in the generated forest as candidate decision rules for Conditional Average Treatment Effect linear decomposition ($\hat{\mathcal{R}}''$). Finally, we discard all the extreme or redundant decision rules (see the Supplementary Materials for details on this filtering).

The filtered set of candidate decision rules $\hat{\mathcal{R}}' \subseteq \hat{\mathcal{R}}''$ is then given in input to the rules selection step. By design, the maximal complexity of the candidate decision rules can be controlled a priori by the maximal length parameter (L) and the other stopping criteria in the tree-ensemble method. The filtering criteria also results very useful in practice to preliminary filter irrelevant decision rules and speed up the rules selection step.

In Figure 2, we present an example of a tree-ensemble estimate to visualize the above-described procedure. The generated forest is composed of $T = 5$ trees and 12 total leaves. They correspond to 11 distinct decision rules ($x_2 \geq 0.6$ is double). Among these, we discard all the not significant rules (in light blue) based on the filtering described above. The remaining 8 leaves in dark blue are the candidate decision rules given in input to the rules selection.

By default, we propose to combine both Random Forest and Gradient Boosting Machine (GBM) for rules generation, following the parameters' setting described by Friedman and Popescu (2008) and Nalenz and Villani (2018).

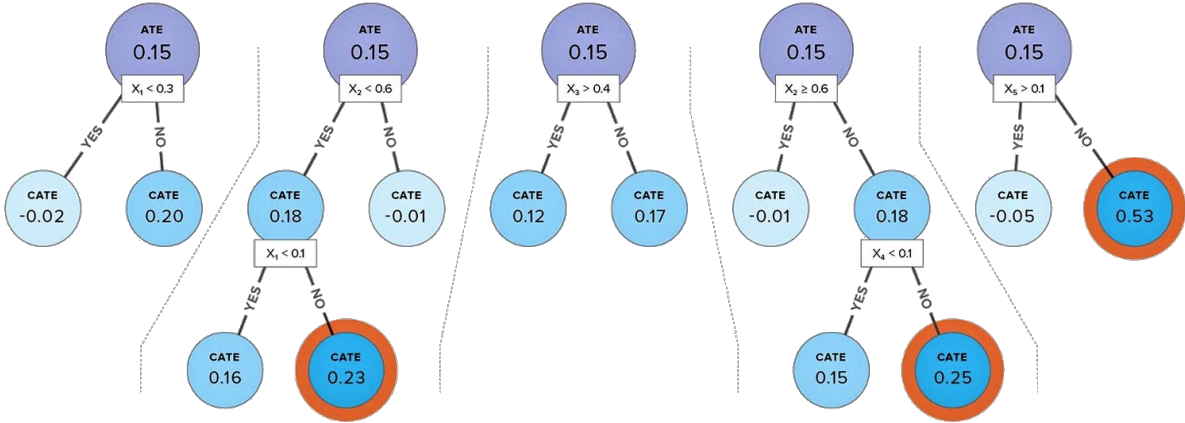


Figure 2: Visual representation of an example of (simple) rule generation and selection procedure. Among the 12 leaves, only the decision rules associated with the 8 leaves in dark blue are considered as candidate decision rules for the rule selection. The 3 leaves highlighted in red represent the decision rules that are finally selected by the stability selection procedure.

3.1.3 Rules Selection

The number of candidate decision rules M' extracted by the rules generation procedure grows exponentially with the maximal length and linearly with respect to the number of trees (before filtering). Although the filtering criteria already discard the not-significant rules, we are not ensuring the stability of these decision rules—i.e., given variations in the discovery set, these rules might be replaced with different ones. To enforce stability in the discovery, we apply a stability selection regularization procedure to extract only the set of robust and predictive decision rules in terms of heterogeneity characterization. To do so, we rely on the following penalized regression for rule selection:

$$\min_{\alpha} \|\tau - (\bar{\tau} + R\alpha)\|_2^2 + \lambda \|\alpha\|_l \quad (3.1)$$

where R is the decision rules matrix, λ is the regularization parameter, and $\|\cdot\|_l$ is a given norm. We select only the rules whose corresponding AATE estimation is different from zero. The least absolute shrinkage and selection operator (LASSO) estimator (Tibshirani; 1996) has been popular and widely used over the past two decades in order to solve the problem in (3.1) with $l = 1$.

The usefulness of this estimator among other penalization regression methods is demonstrated

in various applications (see, e.g., [Su et al.; 2016](#); [Belloni et al.; 2016](#); [Chernozhukov et al.; 2016, 2017](#)). In practice, the true individual (and average) treatment effects are not observed, and we replace them with the corresponding estimates $\hat{\tau}^{dis}$ already computed. We also propose enforcing the discovery of shorter, thus less complex, decision rules, by weighting the columns of the rules matrix by the complexity (length) of the corresponding rule:

$$\tilde{R}_{i,m} = \frac{R_{i,m}}{\text{length}(r_m)} \quad \forall i \in \mathcal{I}^{dis}, \forall m \in \{1, \dots, M'\}. \quad (3.2)$$

Indeed, the same heterogeneity in the treatment effect can be expressed by different sets of decision rules with different complexity. By weighting the columns of the rules matrix by the inverse of the length of the rules, we enforce the discovery of shorter, yet simpler ([Bargagli Stoffi, Cevolani and Gnecco; 2022](#)), characterizations.

When the data is high-dimensional, selecting λ can be challenging ([Hastie et al.; 2015](#)). Stability Selection [Meinshausen and Bühlmann \(2010\)](#) provides a procedure to stably extract the set of decision rules characterizing the heterogeneity of treatment effect controlling for the false discovery. Here, we propose to rework the stability selection procedure as follows.

Let $\mathcal{D}^{dis} = (\hat{\tau}^{dis}, \hat{\mathcal{R}}')$ the discovery subsample individual treatment effect estimations and candidate decision rule estimates. For each value of $\lambda \in \Lambda$, we bootstrap B different subsample $\mathcal{D}_{(b)}$. For each subsample $\mathcal{D}_{(b)}$ a regularized regression—e.g., the model in (3.1)—is run on $\mathcal{D}_{(b)}$ to obtain a selection set $\hat{\mathcal{R}}_{(b)}^\lambda \subseteq \hat{\mathcal{R}}'$ of decision rules. For each candidate decision rule $r_m \in \hat{\mathcal{R}}'$, let π_m^λ its probability of being selected by a certain selection algorithm characterized by λ :

$$\pi_m^\lambda = P\{r_m \in \hat{\mathcal{R}}^\lambda\}, \quad (3.3)$$

estimated by:

$$\hat{\pi}_m^\lambda = \frac{1}{B} \sum_{b=1}^B \mathbb{I}\{r_m \in \hat{\mathcal{R}}_{(b)}^\lambda\}. \quad (3.4)$$

Given an estimate of the selection probabilities for each discovered rule and for each value of λ , we select a stable set of decision rules characterizing heterogeneity in the treatment effect, selecting

all the rules which reached a selection probability bigger than a certain threshold π_{thr} for at least one value of λ :

$$\hat{\mathcal{R}} = \{r_m : \max_{\lambda \in \Lambda} \hat{\pi}_m^\lambda \geq \pi_{\text{thr}}\} \quad (3.5)$$

Meinshausen and Bühlmann (2010) discussed that the solution of stability selection is not sensitive to the initial regularization chosen, which is a desirable feature when selecting decision rules. The authors also state that the empirical results vary little for threshold values $\pi_{\text{thr}} \in (0.6, 0.9)$. The choice of the set of regularization parameters Λ is slightly more challenging than the choice of π_{thr} , but it can be explicitly controlled by an upper bound on the (allowed) per-family error rate (PFER) (see the original paper by Meinshausen and Bühlmann (2010) for further details). In addition to this, controlling for false discoveries is been shown to be of critical importance in the field of heterogeneous treatment effect discovery (Johnson et al.; 2022; Bargagli-Stoffi, De Witte and Gnecco; 2022). By bounding the finite sample probability of making a Type I error, i.e., the probability of discovering a false positive decision rule, stability selection allows to control for the discovery of subgroups that are not likely to substantially contribute to the heterogeneity in the causal effects (we refer to Meinshausen and Bühlmann; 2010, for further details on the finite sample properties of the stability selection methodology). Bodinier et al. (2021) has recently proposed an automated selection of these parameters coming from the maximization of a stability measure.

In Figure 1, we presented an example of an ensemble of trees for rules selection. Among the eight decision rules associated with the terminal nodes in dark blue, the three terminal nodes highlighted in red represent the selected decision rules by the stability selection procedure.

3.2 Inference

Once a set of (robust) decision rules $\hat{\mathcal{R}}$ is estimated from the discovery subsample, we estimate the coefficient of the corresponding treatment effect linear decomposition on the inference subsample \mathcal{I}^{inf} through a two-stage estimation procedure.

3.2.1 Individual Treatment Effect Estimation

First, for each individual $i \in \mathcal{I}^{inf}$, we estimate the corresponding Individual Treatment Effect $\hat{\tau}_i^{inf}$ (pseudo-outcome), relying on Assumption 1-3. Causal Rule Ensemble is model-agnostic with respect to the used ITE estimators, and any algorithm can be used, leading to different convergence properties. Let's observe that it is not required to use the same estimator selected in the discovery step, and certain methods could be preferred to others for one or the other task. For a brief overview of the six ITE estimators compared in the simulations, see the Supplementary material.

3.2.2 Additive Average Treatment Effect Estimation

Then, relying on the linear decomposition of CATE in (4), a two-stage Conditional Average Treatment Effect estimate is given by:

$$\hat{\tau}_i^{inf} = \bar{\tau} + \sum_{m=1}^M \alpha_m \cdot r_m(\mathbf{x}), \quad (3.6)$$

which can be written in matrix form as $\boldsymbol{\tau} = \bar{\tau} + \mathbf{R}\hat{\boldsymbol{\alpha}}$. Equation 3.6 can be used both to characterize vulnerable and resilient subgroups based on the retrieved decision rules and the corresponding AATEs magnitude and sign, as well as to compute the CRE estimate of the (individual) treatment effect over the whole population. The estimate of the Additive Average Treatment Effects (AATEs) can be estimated as:

$$\hat{\boldsymbol{\alpha}} = (\mathbf{R}^T \mathbf{R})^{-1} \mathbf{R}^T (\hat{\boldsymbol{\tau}} - \bar{\boldsymbol{\tau}}), \quad (3.7)$$

Under a few additional conditions, we can prove the consistency and asymptotic normality of the estimator $\hat{\boldsymbol{\alpha}}$.

3.2.3 Statistical Properties

Proposition 1. *Let $\hat{\boldsymbol{\tau}}$ a consistent estimator for $\boldsymbol{\tau}$ (i.e., AIPW). Under the Treatment Effect linear decomposition Assumption (Condition 1) and assuming $\mathbb{E}(\mathbf{R}^T \mathbf{R}) = \mathbf{Q}$ is a positive definite matrix (Condition 2), the Additive Average Treatment Effects estimator $\hat{\boldsymbol{\alpha}} = (\mathbf{R}^T \mathbf{R})^{-1} \mathbf{R}^T (\hat{\boldsymbol{\tau}} - \bar{\boldsymbol{\tau}})$ is a consistent estimator for $\boldsymbol{\alpha}$.*

[See proof in Appendix C]

Three additional assumptions are required to prove the asymptotic normality of the estimator $\hat{\boldsymbol{\alpha}}$:

3. $\mathbb{E}(\mathbf{R}_{ij}^4) < \infty \quad \forall i \in \mathcal{I}^{inf} \text{ and } \forall j \in \{1, \dots, M\};$
4. $\mathbb{E}(\nu_i^4) < \infty \quad \forall i \in \mathcal{I}^{inf};$
5. $\mathbb{E}(\nu_i^2 \mathbf{R}_i^T \mathbf{R}_i) = \Omega \succ 0$ (positive definite) $\forall i \in \mathcal{I}^{inf}.$

where \mathbf{R}_i represents the i -th row of the rules matrix R . Since R is a binary matrix, Condition (3) is satisfied by design. The following theorem represents the asymptotic distribution of $\hat{\boldsymbol{\alpha}}$.

Proposition 2. *If Conditions (1)-(5) hold, then*

$$\sqrt{N}(\hat{\boldsymbol{\alpha}} - \boldsymbol{\alpha}) \xrightarrow{d} \mathcal{N}(0, V) \text{ as } N \rightarrow \infty \quad (3.8)$$

where $V = Q^{-1}\Omega Q^{-1}$.

[See proof in Appendix C]

A variance-covariance matrix estimator $\hat{V} = \hat{Q}^{-1}\hat{\Omega}\hat{Q}^{-1}$ can be obtained by the sandwich formula where:

$$\hat{Q} = \frac{R^T R}{N}, \quad (3.9)$$

$$\hat{\Omega} = \frac{\boldsymbol{\nu}^T R R^T \boldsymbol{\nu}}{N} \quad (3.10)$$

$$\hat{\boldsymbol{\nu}} = \hat{\boldsymbol{\tau}} - (\hat{\boldsymbol{\tau}} + R\boldsymbol{\alpha}) \quad (3.11)$$

This estimator is robust and often referred to as White's estimator (White; 1980). There are other approaches to obtain a heteroscedasticity consistent covariance matrix as discussed in Long and Ervin (2000). For small samples, Efron's estimator (Efron; 1982), known as the HC3 estimator, can be considered alternatively. Also, if the variance σ_i^2 is known from the large sample properties

of existing methods for obtaining $\hat{\tau}_i^{inf}$, then feasible generalized least squares estimators (Lewis and Linzer; 2005) can be considered. Given an estimate of the covariance-variance matrix, we also provide an (asymptotic) confidence interval for each Additive Average Treatments Effect α_m .

4 Simulations

To assess the relative performance of CRE, we carried out two simulation studies. In the first simulation study, we assess the algorithm’s performance in heterogeneity characterization, retrieving the correct effect modifiers and decision rules. We compare different variants of CRE using different ITE estimators, and we evaluate them with different magnitudes of the causal effect.

In the second simulation study, we benchmark the estimation accuracy of CRE. We compare the CRE estimator with state-of-the-art methodology for the estimation of HTE. We also verify empirically the consistent estimation of the AATEs (Proposition 1).

We consider several data-generating processes, varying the confounding mechanism, sample size, and the number and complexity of the rules. In this section, we report the main results of both analyses; for a complete overview of the results with all the variant data-generating processes, see the Supplementary Material.

4.1 Heterogeneity Discovery

Let \mathcal{I} a sample of $N = 2,000$ individuals. For each individual $i \in \mathcal{I}$, let’s define: $X_i^1, \dots, X_i^p \stackrel{\text{iid}}{\sim} \text{Bernoulli}(0.5)$, and $Z_i \sim \text{Bernoulli}(\pi_i)$ with $\pi_i = \frac{1}{1+e^{+1-X_i^1+X_i^2-X_i^3}}$ where \mathbf{X}_i is the vector of the $p = 10$ observed (binary) covariates of individual i , and Z_i represents its assigned (binary) treatment. Let us further define the potential outcomes as

$$Y_i(0) \sim \mathcal{N}(\mu_i^0, 1) \quad \text{with} \quad \mu_i^0 = X_i^1 + X_i^3 + X_i^4 + k \cdot \mathbb{1}_{\{x_1=1; x_2=0\}}(\mathbf{X}_i),$$

and

$$Y_i(1) \sim \mathcal{N}(\mu_i^1, 1) \quad \text{with} \quad \mu_i^1 = X_i^1 + X_i^3 + X_i^4 + k \cdot \mathbb{1}_{\{x_5=1; x_6=0\}}(\mathbf{X}_i)$$

where $k \in \mathbb{R}$ represents the magnitude of the causal effect. It follows that the (unobserved) treatment effect for individual i is equal to: $\tau_i = Y_i(1) - Y_i(0) = -k \cdot \mathbb{1}_{\{x_1=1;x_2=0\}}(\mathbf{X}_i) + k \cdot \mathbb{1}_{\{x_5=1;x_6=0\}}(\mathbf{X}_i) + \nu_i$ where $\nu_i \sim \mathcal{N}(0, 2)$ is an additive zero-mean noise. With $M = 2$ decision rules, $\bar{\tau} = 0$, $r_1(\mathbf{x}) = \mathbb{1}_{\{x_1=1;x_2=0\}}(\mathbf{x})$, $r_2(\mathbf{x}) = \mathbb{1}_{\{x_5=1;x_6=0\}}(\mathbf{x})$, $\alpha_1 = \alpha_2 = k$, and $\tau(\mathbf{x}) = -k \cdot \mathbb{1}_{\{x_1=1;x_2=0\}}(\mathbf{x}) + k \cdot \mathbb{1}_{\{x_5=1;x_6=0\}}(\mathbf{x}) = \sum_{m=1}^M \alpha_m \cdot r_m(\mathbf{x})$.

We measure the CRE’s capability in retrieving both the true effect modifiers (i.e., x_1, x_2, x_5, x_6) and the exact decision rules (i.e., r_1, r_2) varying the magnitude of the causal effect (i.e., k). Let \mathcal{S} be the set of true effect modifiers (or decision rules) and $\hat{\mathcal{S}}$ the set discovered by CRE. We define first: $TP = |\hat{\mathcal{S}} \cap \mathcal{S}|$, $FP = |\hat{\mathcal{S}} - \mathcal{S}|$, $FN = |\mathcal{S} - \hat{\mathcal{S}}|$, where TP represents the number of elements properly retrieved, FP represents the number of elements wrongly retrieved, and FN represents the number of right elements not retrieved. We can then define: $\text{Recall} = \frac{TP}{TP+FN}$, $\text{Precision} = \frac{TP}{TP+FP}$, $\text{F1-score} = 2 \cdot \frac{\text{Recall} \cdot \text{Precision}}{\text{Recall} + \text{Precision}}$, where *Recall* is the ratio of true elements properly retrieved (quantitative performance), *Precision* is the ratio of correct elements retrieved (qualitative performance), and the *F1-score* combines these 2 measures in a harmonic mean.

We consider six variants of CRE with six distinct ITE estimators: Augmented Inverse Probability Weighting (AIPW), Bayesian Causal Forest (BCF), Causal Bayesian Additive Regression Trees (Causal BART), S-Learner, T-Learner, and X-Learner (see the Supplementary Material for a complete overview of these methods). For each variant of CRE and causal effect size k , we compare the mean Recall, Precision, and F1-score and their corresponding 95% confidence intervals over 250 Monte Carlo experiments.

In Table E.1 in the Supplementary Material, we summarize the Causal Rule Ensemble’s method parameters and the hyperparameters used for this analysis. The results are reported in Figure 3. As expected, both effect modifiers retrieval and decision rules retrieval metrics increase monotonically with respect to the causal effect size k . All the method variants perform similarly for effect modifiers retrieval, and all the variants reach almost perfect discovery by $k = 3$. Decision rule discovery is more challenging due to the larger hypothesis space. Indeed, in the case of binary covariates (current setting), the number of possible decision rules is equal to: $\sum_{l=1}^L \binom{p}{l} \cdot 2^l$ growing exponentially with maximum rules’ length L . and even more in the setting of discrete or continuous covariates,

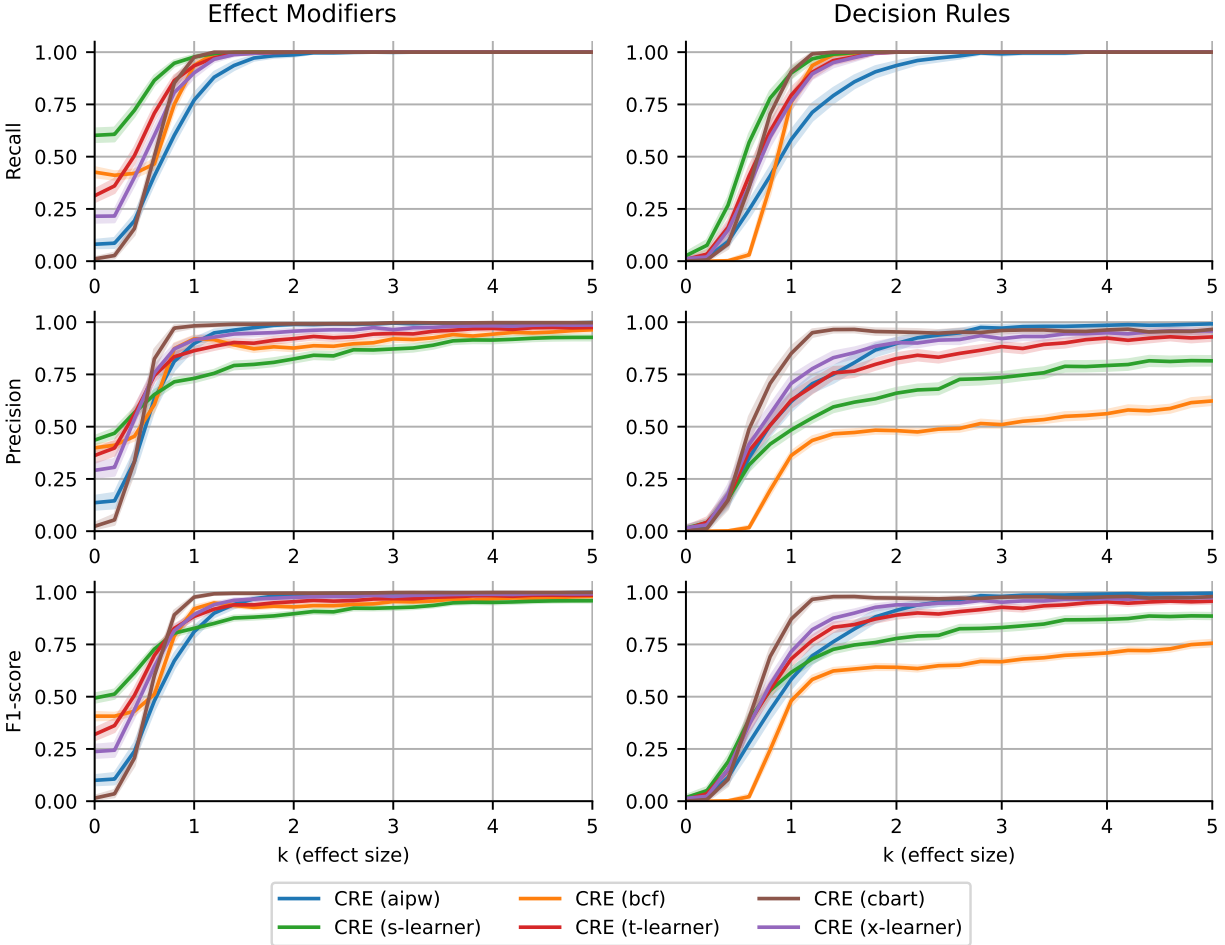


Figure 3: Simulation study for heterogeneity discovery results with 2 rules, linear confounders, and 2,000 observations. Mean *Precision*, *Recall* and *F1-score* (lines) with the corresponding 95% confidence intervals (bands) over 250 Monte Carlo experiments are reported for each method and causal effect size k . For each CRE variant, the heterogeneity characterization discovery converges (with respect to effect size) to the true heterogeneity characterization.

depending on the discretization criteria in the rules generation.

All the method variants retrieve all the true decision rules ($\text{Recall} = 1$) by $k = 3$, but a few variants (i.e., BCF and S-Learner) also keep retrieving additional redundant rules ($\text{Precision} \ll 1$) even for $k > 3$. This drawback can be addressed by fine-tuning the strength in the Rules Selection step (e.g., increasing cutoff π_{thr} , or reducing the PFER in the Stability Selection), which we kept constant for all the methods for a fair comparison. Causal Rule Ensemble based on Causal BART, AIPW, T-Learner, and X-Learner for ITE estimation leads to a more stable and precise rules

discovery. In agreement with the literature (Hill; 2011), Causal Rule Ensemble based on Causal BART works better than any other variants for small effect sizes.

Consistent results are obtained when varying: (i) the sample size (1,000, 2,000, 5,000); (ii) the number of the decision rules (2, 4); (iii) the complexity of the decision rules (1, 2, 3); (iv) the type of confounding (none, linear, non-linear). A comprehensive analysis of these additional simulations is reported in the Supplementary Material.

4.2 Heterogeneous Treatment Effect Estimation

The simulation study on the heterogeneous effect estimation follows the same data-generating process described in Section 4.1. For each method, we evaluate the mean and standard deviation Root-Mean-Square Error (RMSE) and Bias on ITE estimation over 250 Monte Carlo experiments per method. We consider the same six variants of CRE with the following ITE estimators: Bayesian Causal Forest (BCF), Causal Bayesian Additive Regression Trees (Casual BART), S-Learner, T-Learner, and X-Learner; and we compare them with the same “standalone” ITE estimators, which are commonly recognized among the best-performing algorithms for heterogeneous treatment effect estimation. We report the results in Table 1.

Method	RMSE		Bias	
	μ	σ	μ	σ
CRE (AIPW)	0.1336	0.0603	0.0016	0.0891
CRE (BCF)	0.1482	0.0558	0.0047	0.0795
CRE (S-Learner)	0.1494	0.0589	0.0017	0.0860
CRE (T-Learner)	0.1495	0.0649	0.0011	0.0937
CRE (X-Learner)	0.1466	0.0659	0.0010	0.0937
CRE (Causal BART)	0.1398	0.0625	0.0009	0.0816
AIPW	2.0807	0.1919	0.0032	0.0562
BCF	0.1339	0.0373	0.0042	0.0522
S-Learner	0.4837	0.0334	0.0020	0.0532
T-Learner	0.8065	0.0373	0.0035	0.0573
X-Learner	1.1878	0.0291	0.0035	0.0573
Causal BART	0.9925	0.0163	0.0020	0.0520

Table 1: Simulation study for (heterogeneous) treatment effect estimation, with $M = 2$ rules, linear confounder, 2,000 individuals and under CATE linear decomposition assumption. For all the methods, the mean (μ) and standard deviation (σ) treatment effect root mean squared error (RMSE) and bias (Bias) over 250 Monte Carlo experiments are reported.

Overall, CRE outperforms the corresponding ‘standalone’ ITE estimators. In particular, CRE (AIPW), CRE (S-Learner), CRE (T-Learner), CRE (X-Learner), and CRE (Causal BART) significantly outperform the corresponding AIPW, S-Learner, T-Learner, X-Learner, Causal BART estimators for ITE estimation, and CRE (BCF) and BCF lead to comparable performances. Among the ‘standalone’ ITE estimators, BCF is the method with the largest Bias (> 0.04). Our hypothesis is that its corresponding errors in ITE estimation in the CRE discovery step lead to incorrect heterogeneity characterization, propagating the error at the estimation time.

In Figure 4 we report a boxplot of the AATEs (α) estimation bias ($\text{Bias}(r_m) = \alpha_m - \hat{\alpha}_m$) for all $r_m \in \mathcal{R}$) comparing the different CRE variants over the same 250 Monte Carlo experiments.

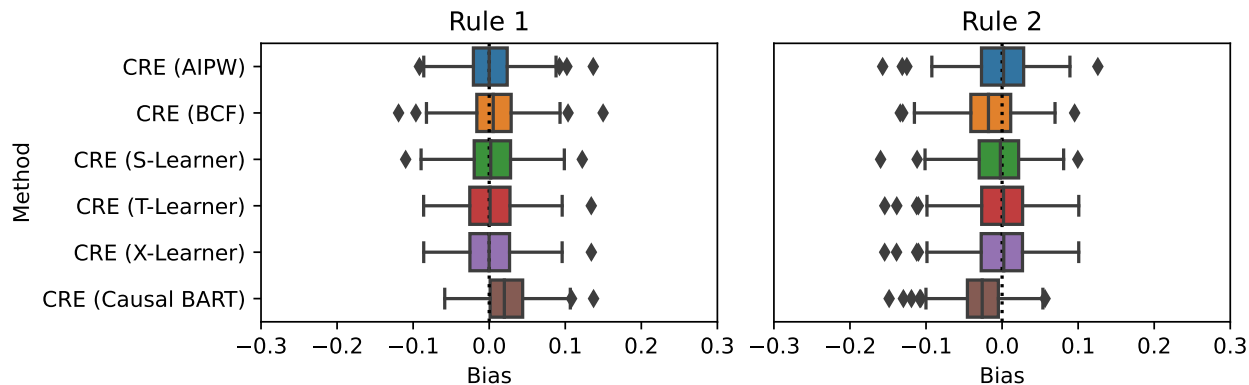


Figure 4: Simulation study for (heterogeneous) treatment effect estimation, with $M = 2$ rules, linear confounding and 2,000 individuals. For all the CRE variants, for each rule, the AATE’s bias over 250 Monte Carlo experiments is reported in a boxplot.

As expected from Proposition 1, all the CRE variants lead to consistent AATEs estimation (median centered in 0), even without assuming perfect rules discovery. Consistent results for ITE, ATE, and AATE estimation are obtained in varying: (i) the sample size (1,000, 2,000, 5,000); (ii) the number of the decision rules (2, 4); (iii) the complexity of the decision rules (1, 2, 3); (iv) the type of confounding (none, linear, non-linear). A comprehensive analysis and discussion of these additional simulations are reported in the Supplementary Material.

5 Heterogeneous Effects of Air Pollution Exposure on Mortality

The literature indicates that long-term exposure to lower levels of $\text{PM}_{2.5}$ is associated with a significant decrease in mortality (see [Carone et al.; 2020](#), for a review). While previous research has contributed to understanding the average treatment effect of long-term $\text{PM}_{2.5}$ exposure, it has largely neglected to explore potential heterogeneity in the causal effects. However, it is essential to investigate how the causal effect may differ across different groups of individuals in health studies to develop more effective health policies.

In this context, our focus is on identifying vulnerability or resilience in the causal effects with respect to the average effect of exposure to air pollution on mortality. In particular, we examine the heterogeneous effects of long-term $\text{PM}_{2.5}$ exposure to high levels of air pollution among individuals aged 65 and above who were enrolled in Medicare in the years 2010-2016. By utilizing our CRE methodology, we showcase how our approach can identify distinct groups, estimate the heterogeneity in the effects of long-term $\text{PM}_{2.5}$ exposure on mortality, and identify the social-economical characteristics that distinguish the different heterogeneous subgroups.

5.1 Data

We collected data from 35,331,290 Medicare beneficiaries across the contiguous U.S. For each beneficiary, we have information on age, sex, race (specifically categorized as Hispanic, black, white, and other race), eligibility for Medicaid (this variable is a proxy of low social-economic status), and whether or not they died in the 5 follow-up years (2012-2016). We integrated these data with average $\text{PM}_{2.5}$ levels in 2010 and 2011. Figure 5 depicts the average levels $\text{PM}_{2.5}$ for the biennium 2010-2011 across the contiguous U.S.

Furthermore, we integrated census variables at the ZIP code level and county-level variables. At the ZIP code level, we have information on the average household income, average home value, the proportion of residents in poverty, the proportion of residents without a high school diploma, the population density, the proportion of residents who own their houses and the proportion of the black and Hispanic population. Furthermore, we considered meteorological data such as the average maximum daily temperatures and relative humidity during summer (June to September)

and winter (December to February). At the county level, we considered variables on the average body mass index and the average smoking rate.

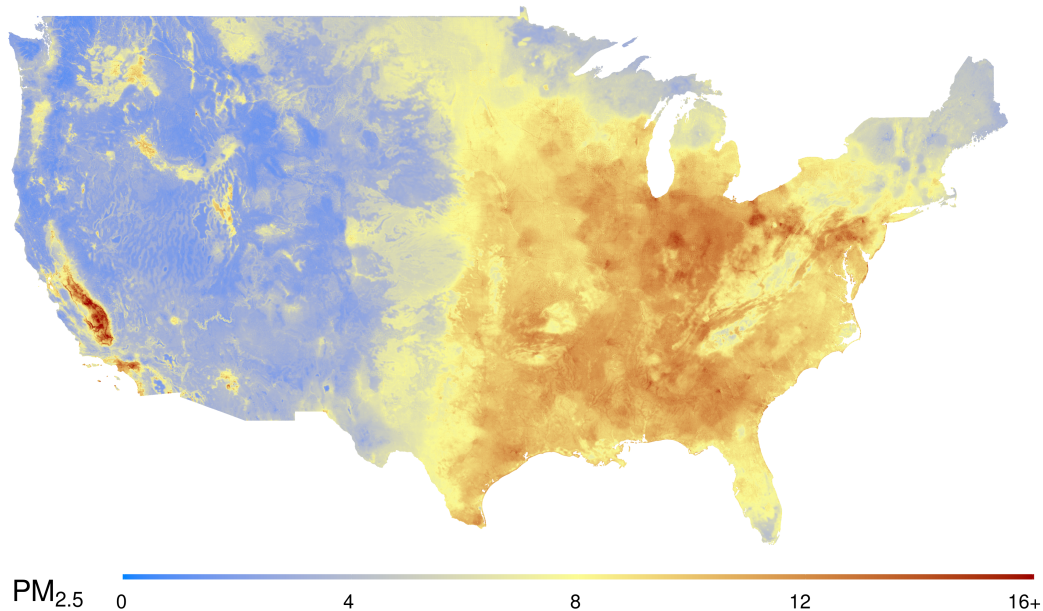


Figure 5: Average levels $PM_{2.5}$ for the biennium 2010-2011 in the contiguous U.S.

5.2 Study Design

We define the treatment variable as $Z = 1$ if the average $PM_{2.5}$ in 2010 and 2011 is above the threshold of $12\mu g/m^3$ and $Z = 0$ otherwise. The choice of $12\mu g/m^3$ as a threshold aligns with the current National Ambient Air Quality Standard (NAAQS) established by the Environmental Protection Agency (EPA). All the covariates at the individual level (except for age) are already binary, and we keep them as such. In order to enforce interpretability, we also binarize all the other covariates—i.e., age, zip code level variables, and county level variables—using the median as a threshold. Different discretization criteria and thresholds can be considered for more detailed heterogeneity characterization (even not discretization at all). For each individual, the observed factual outcome Y is equal to 1 if the person died in the five follow-up years (2012-2016) and 0 otherwise.

We investigate the heterogeneity in the effects of air pollution on mortality in the four different

geographical regions defined by the U.S. Census Bureau separately (see Figure F.1). It is crucial to investigate the effects of air pollution on health across the different geographical regions of the U.S. for several reasons.

Firstly, the U.S. is a vast country with a diverse climate and environmental conditions, leading to substantial differences in air quality and exposure to air pollution across different regions (see Figure 5). As highlighted by [Baxter et al. \(2013\)](#), it is utterly important to assess the differential risks of air pollution on mortality at a regional level as they could be suggestive heterogeneous health responses driven by variations in the $PM_{2.5}$ composition and the concentration of gaseous pollutants.

Secondly, people living in different regions may have different susceptibilities to the health effects of air pollution due to various factors such as genetics, lifestyle, and pre-existing health conditions ([Kloog et al.; 2013](#); [Zanobetti et al.; 2009](#)). Therefore, understanding the heterogeneity in the health effects of air pollution across different regions can help identify vulnerable populations and design targeted interventions to mitigate the adverse health effects.

Thirdly, [Dedoussi et al. \(2020\)](#) found that 41 to 53% of air-quality-related premature mortality resulting from a state’s emissions occurs outside that state. Hence, regional-level analyses—factoring in the potential out-of-state sources of emission—directly map into region-wide policies that may be more effective in reducing the mortality burdens from exposure to air pollution.

All this considered, investigating the effects of air pollution on health across different regions of the U.S. is essential for identifying the specific risks associated with exposure to pollutants, understanding the heterogeneity in the health effects across different populations, and informing public health policies and interventions.

The list of CRE methods and hyper-parameters used in these analyses is reported in Table E.2 in the Supplementary Material.

5.3 Results

Consistently with the literature, we found that being exposed to higher levels of air pollution with respect to the NAAQS of $12\mu g/m^3$ leads to an increase in mortality in each of the four regions of the

contiguous U.S. considered. The greatest increase was found in the Northeast, where individuals exposed, in the biennium 2010-2011, to levels of $PM_{2.5}$ higher than the NAAQS were found to be 16.2% more likely to die in the five following years, compared to those exposed to levels lower than the NAAQS. We found 14.9%, 7.1%, and 2.3% increases in mortality in the West, Midwest, and South, respectively.

Using CRE, next to the average treatment effects, we were also able to discover notable heterogeneity with respect to the average treatment effect in each of the four regions. Figure 6 depicts the results of our analyses.

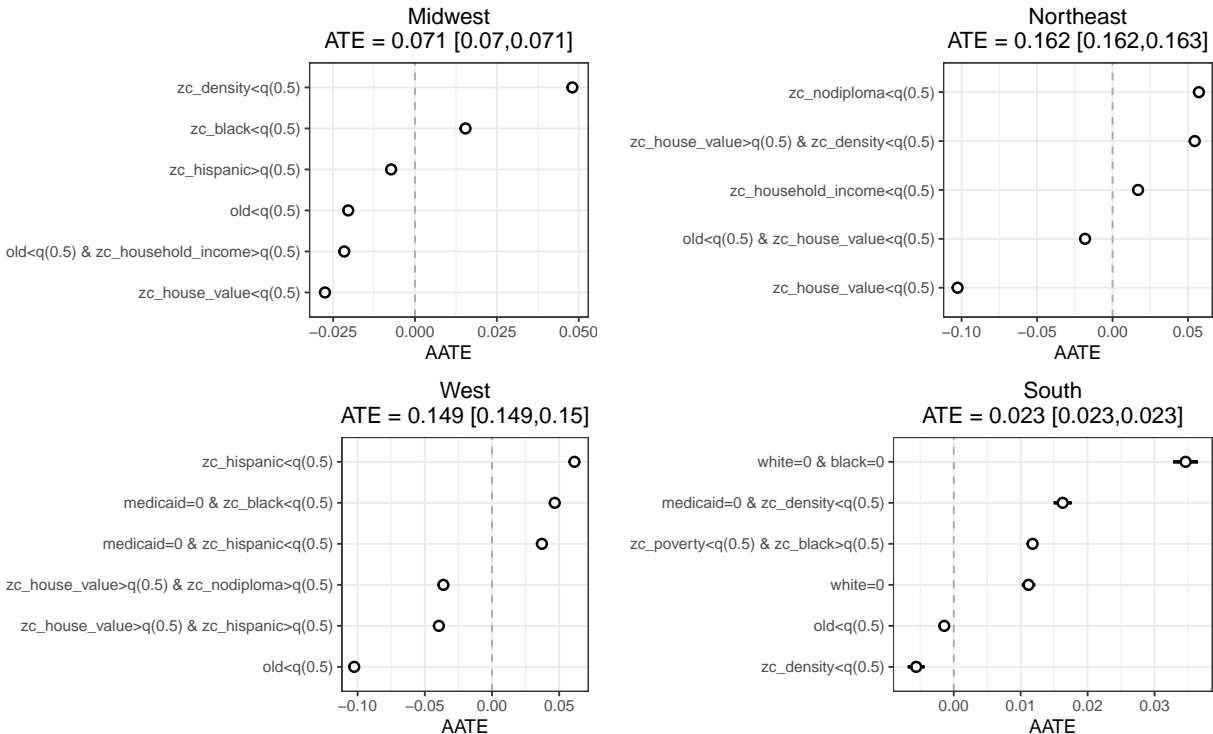


Figure 6: Results obtained from CRE for the discovery and estimation of HTE of air pollution exposure on mortality. For each U.S. Census geographical region, we report the ATE and the various AATEs for the discovered decision rules (with the corresponding 95% confidence interval). The prefix *zc* in the variable names stands for zip-code level variable, and *county* stands for county level. All the other variables are at the individual level. The threshold $q(\alpha)$ stands for the α -quantile of that variable in that region—e.g., $q(0.5)$ is the median.

For each of the four regions, we found both positive and negative additive average treatment effects. When an AATE is positive, it means that, under that decision rule, it was estimated a

treatment effect greater than without (fixing all the others' contributions). Conversely, when an AATE is lower than zero, it means that, under that decision rule, it was estimated a treatment effect smaller than without. Notably, for all the regions, the effects of the AATEs never completely offset the ATE, indicating an overall detrimental impact of exposure to higher levels of air pollution on health both at a population and a subgroup level.

We find high fragmentation in the heterogeneity characterizing the groups where exposure to higher levels of PM_{2.5} increases the mortality rate—i.e., a positive AATE. A clear trend is provided by an increased risk for individuals living in low-density areas (i.e., `zc_density` < $q(0.5)$) in the Northeast, Midwest, and South. Low-density areas, such as rural areas, can be characterized by decreased access to medical care, and this, paired with exposure to higher levels of air pollution, may be a possible driver of higher vulnerability. The second notable heterogeneity driver comes from individuals with a low socio-economic status (i.e., `medicaid` = 0) or living in low-income areas (i.e., `zc_household_income` < $q(0.5)$) in the West and South being more vulnerable. The last one is for individuals living in zip codes with the percentage of the black population higher than the median (i.e., `zc_black` > $q(0.5)$), yet less poor (i.e., `zc_poverty` < $q(0.5)$), areas in the South being more vulnerable. Other vulnerabilities are found in individuals living in areas with a smaller black population (in the Midwest), a smaller rate of people without a diploma (in the Northeast), a smaller Hispanic population (in the West), and people neither white nor black (in the South).

In juxtaposition, the groups where exposure to higher levels of PM_{2.5} decreases the ATE on the mortality rate are mainly composed of a population with fewer old individuals (in particular in the Midwest, West, and South). Consistently, with what was found for the vulnerability, individuals living in areas with a higher density of minority groups (i.e., Hispanic in the Midwest and West) were found to be at lower risk. While surprising this has already been documented in the literature (Liu et al.; 2021), and it finds a possible explanation in potential survival bias (see, e.g., Mayeda et al.; 2018; Shaw et al.; 2021). Survival bias happens in cohort studies that start at a late stage in people's lives, leading to the most vulnerable individuals in certain groups dying before entering the cohort. In this case, the individuals entering the cohort are the most resilient ones and might depict a lower mortality risk, with respect to the average risk, even when exposed to higher levels

of pollutants (Liu et al.; 2021). This is likely to be the case for these groups. We know, from previous literature, that Hispanic and black populations are structurally exposed to higher levels of air pollution. Exposure effects might accumulate over time—as is likely the case with $\text{PM}_{2.5}$ —leading to the most fragile individual dying before entering the Medicare cohort (see, e.g., Pope III et al.; 2019).

To conclude, CRE was able to identify the key factors in the population characteristics that explain different degrees of vulnerability to exposure to air pollution. This application demonstrates the ability of CRE to retrieve non-trivial yet interpretable characterization of the heterogeneous subgroups.

6 Conclusion

In this paper, we introduced a new method for interpretable discovery and estimation of heterogeneous treatment effects. The proposed CRE methodology accommodates the well-known shortcomings in the flexibility of (individual) causal trees and interpretability of ensembles of causal trees (i.e., Causal Forest) relying on the linear decomposition of the treatment effect in terms of decision rules. By design (see Stability Selection), its heterogeneity discovery is stable to sample-to-sample variations, and under the assumptions of identifiability and linear decomposition, CRE leads to consistent estimates.

The decision rules characterizing the heterogeneity are estimated by a *fit-the-fit* procedure, relying on a preliminary individual treatment effect (pseudo-outcome) estimation by any existing treatment effect estimator. Similarly, the final linear model relies on an analogous preliminary individual treatment effect (pseudo-outcome) estimation. Therefore, the CRE method can be thought of as a *refinement* process of the outputs produced by existing methods. Different properties characterize different estimators, and the performance of CRE varies with respect to them. If an estimator properly estimates the heterogeneity in the treatment effect, the CRE method discovers the underlying treatment effect structure with higher probability and represents this structure in an easy-to-interpret form.

The maximal number and complexity of the rules can be set by researchers or practitioners.

Indeed, a few simple (i.e., not lengthy) rules are utterly important for public policy implications, where policy guidelines need to be as simple and as general as possible. However, when it comes to precision medicine, discovering a possibly lengthy rule that is specific to a patient could be of interest. Also, the choice of how many causal rules to discover in the discovery step may depend on the questions that practitioners want to answer. For example, policymakers generally want to discover a short list of risk factors. A few important subgroups defined by the risk factors are usually easy-to-understand and further foster focused discussions about the assessments of potential risks and benefits of policy actions. Due to the restriction of resources, public health can be promoted efficiently when prioritized subgroups are available. Conversely, in precision medicine, a comparatively larger set of decision rules can be chosen. Indeed, an important goal is to identify patient subgroups that respond to treatment at a much higher (or lower) rate than the average (Loh et al.; 2019). Also, identifying a subgroup that must avoid the treatment due to its excessive side effects can be valuable information. However, discovering only a few subgroups is likely to miss this extreme subgroup.

From simulations, we exhibited that CRE has competitive performances both in the discovery and estimation of the treatment effect. We showed first, as a proof of concept, that under the linear decomposition assumption and significant causal effect, CRE perfectly retrieves the correct treatment effect decomposition. Then we compared CRE performances in estimation with several of the most successful causal machine-learning methods for heterogeneous treatment effect estimation. Under linear decomposition assumption, CRE significantly outperforms all the other estimators, correctly capturing the heterogeneity in the treatment effect in terms of decision rules. All the simulation studies are repeated with different data-generating processes, leading to consistent results; and numerous seeds to enforce reproducibility.

The use of CRE allowed for the identification of crucial factors in characteristics that help explain the varying levels of susceptibility to air pollution exposure in the elderly population in the U.S. By employing CRE, a non-trivial and comprehensible characterization of distinct subgroups has been retrieved. This application not only showcased the efficacy of CRE in deciphering complex patterns in data but also highlighted the significance of understanding the heterogeneous nature

of populations in relation to environmental hazards. Such insights should be paired with extensive analyses of vulnerability to air pollution in the younger population. The results of our analyses found indeed that there may be room for possible survival bias when analyzing the vulnerability to air pollution due to structural differences in air pollution exposure across the U.S.

A number of extensions of the CRE method can be possible. CRE deals with the exploration of heterogeneous treatment effects in the simple case of a binary treatment in a cross-sectional setting. It would be of great interest to extend the CRE setting to continuous treatment effects and time-series studies, as these dimensions might be critically important for a number of applications in social and health sciences. Furthermore, starting from CRE to develop interpretable methods for optimal policies or targeted treatment assignment is also crucial. Optimal policies involve assigning treatments to individuals in a manner that maximizes the desired outcome while taking into account their unique characteristics. Such an approach could lead to more effective and efficient treatment outcomes, reduce unnecessary treatment and improve patient outcomes. Additionally, by targeting treatments to the appropriate individuals, optimal policies can help reduce health disparities and ensure that interventions are more equitably distributed. Therefore, developing methods for optimal policies is an important future extension of CRE in the direction of moving one more step closer to achieving personalized and effective healthcare.

References

- Athey, S. and Imbens, G. (2016). Recursive partitioning for heterogeneous causal effects, *Proceedings of the National Academy of Sciences* **113**(27): 7353–7360.
- Athey, S., Tibshirani, J., Wager, S. et al. (2019). Generalized random forests, *The Annals of Statistics* **47**(2): 1148–1178.
- Bargagli Stoffi, F. J., Cevolani, G. and Gnecco, G. (2022). Simple models in complex worlds: Occam’s razor and statistical learning theory, *Minds and Machines* **32**(1): 13–42.
- Bargagli-Stoffi, F. J., De Witte, K. and Gnecco, G. (2022). Heterogeneous causal effects with imperfect compliance: a bayesian machine learning approach, *The Annals of Applied Statistics* **16**(3): 1986–2009.
- Bargagli-Stoffi, F. J. and Gnecco, G. (2020). Causal tree with instrumental variable: An extension

- of the causal tree framework to irregular assignment mechanisms, *International Journal of Data Science and Analytics* **9**: 315–337.
- Bargagli-Stoffi, F. J., Tortù, C. and Forastiere, L. (2020). Heterogeneous treatment and spillover effects under clustered network interference, *arXiv preprint arXiv:2008.00707* .
- Baxter, L. K., Duvall, R. M. and Sacks, J. (2013). Examining the effects of air pollution composition on within region differences in pm_{2.5} mortality risk estimates, *Journal of Exposure Science & Environmental Epidemiology* **23**(5): 457–465.
- Belloni, A., Chernozhukov, V., Hansen, C. and Kozbur, D. (2016). Inference in high-dimensional panel models with an application to gun control, *Journal of Business & Economic Statistics* **34**(4): 590–605.
- Bodinier, B., Filippi, S., Nost, T. H., Chiquet, J. and Chadeau-Hyam, M. (2021). Automated calibration for stability selection in penalised regression and graphical models: a multi-omics network application exploring the molecular response to tobacco smoking, *arXiv preprint arXiv:2106.02521* .
- Breiman, L. (1996). Heuristics of instability and stabilization in model selection, *The annals of statistics* **24**(6): 2350–2383.
- Breiman, L. (2001). Random forests, *Machine Learning* **45**(1): 5–32.
- Carone, M., Dominici, F. and Sheppard, L. (2020). In pursuit of evidence in air pollution epidemiology: the role of causally driven data science, *Epidemiology* **31**(1): 1–6.
- Chen, T. and Guestrin, C. (2016). Xgboost: A scalable tree boosting system, *Proceedings of the 22nd ACM SIGKDD international conference on knowledge discovery and data mining*, pp. 785–794.
- Chernozhukov, V., Chetverikov, D., Demirer, M., Duflo, E., Hansen, C. and Newey, W. (2017). Double/debiased/neyman machine learning of treatment effects, *American Economic Review* **107**(5): 261–65.
- Chernozhukov, V., Escanciano, J. C., Ichimura, H., Newey, W. K. and Robins, J. M. (2016). Locally robust semiparametric estimation, *arXiv preprint arXiv:1608.00033* .
- Chipman, H. A., George, E. I. and McCulloch, R. E. (2010). BART: Bayesian additive regression trees, *The Annals of Applied Statistics* **4**(1): 266–298.
- Cox, D. R. (1975). A note on data-splitting for the evaluation of significance levels, *Biometrika* **62**(2): 441–444.
- Crump, R. K., Hotz, V. J., Imbens, G. W. and Mitnik, O. A. (2008). Nonparametric tests for treatment effect heterogeneity, *The Review of Economics and Statistics* **90**(3): 389–405.
- Dedoussi, I. C., Eastham, S. D., Monier, E. and Barrett, S. R. (2020). Premature mortality related to united states cross-state air pollution, *Nature* **578**(7794): 261–265.

- Deng, H. (2019). Interpreting tree ensembles with intrees, *International Journal of Data Science and Analytics* **7**(4): 277–287.
- Di, Q., Wang, Y., Zanobetti, A., Wang, Y., Koutrakis, P., Choirat, C., Dominici, F. and Schwartz, J. D. (2017). Air pollution and mortality in the Medicare population, *New England Journal of Medicine* **376**(26): 2513–2522.
- Dwivedi, R., Tan, Y. S., Park, B., Wei, M., Horgan, K., Madigan, D. and Yu, B. (2020). Stable discovery of interpretable subgroups via calibration in causal studies, *International Statistical Review* **88**: 135–178.
- Efron, B. (1982). *The jackknife, the bootstrap, and other resampling plans*, Vol. 38, Philadelphia, PA: Society for Industrial and Applied Mathematics.
- Foster, J. C., Taylor, J. M. and Ruberg, S. J. (2011). Subgroup identification from randomized clinical trial data, *Statistics in Medicine* **30**(24): 2867–2880.
- Freedman, D. A. (1999). Ecological inference and the ecological fallacy, *International Encyclopedia of the social & Behavioral sciences* **6**(4027-4030): 1–7.
- Friedman, J. H. (2001). Greedy function approximation: a gradient boosting machine, *The Annals of Statistics* **29**(9): 1189–1232.
- Friedman, J. H. and Popescu, B. E. (2008). Predictive learning via rule ensembles, *The Annals of Applied Statistics* **2**(3): 916–954.
- Hahn, P. R., Murray, J. S., Carvalho, C. M. et al. (2020). Bayesian regression tree models for causal inference: regularization, confounding, and heterogeneous effects, *Bayesian Analysis* .
- Hansotia, B. and Rukstales, B. (2002). Incremental value modeling, *Journal of Interactive Marketing* **16**(3): 35–46.
- Hastie, T., Tibshirani, R., Friedman, J. H. and Friedman, J. H. (2009). *The elements of statistical learning: data mining, inference, and prediction*, Vol. 2, Springer.
- Hastie, T., Tibshirani, R. and Wainwright, M. (2015). *Statistical learning with sparsity: the lasso and generalizations*, CRC press.
- Hill, J. L. (2011). Bayesian nonparametric modeling for causal inference, *Journal of Computational and Graphical Statistics* **20**(1): 217–240.
- Holland, P. W. (1986). Statistics and causal inference, *Journal of the American Statistical Association* **81**(396): 945–960.
- Horvitz, D. G. and Thompson, D. J. (1952). A generalization of sampling without replacement from a finite universe, *Journal of the American statistical Association* **47**(260): 663–685.
- Imai, K., Ratkovic, M. et al. (2013). Estimating treatment effect heterogeneity in randomized program evaluation, *The Annals of Applied Statistics* **7**(1): 443–470.
- Jacob, D. (2019). Group average treatment effects for observational studies, *arXiv preprint arXiv:1911.02688* .

- Johnson, M., Cao, J. and Kang, H. (2022). Detecting heterogeneous treatment effects with instrumental variables and application to the oregon health insurance experiment, *The Annals of Applied Statistics* **16**(2): 1111–1129.
- Kennedy, E. H. (2020). Optimal doubly robust estimation of heterogeneous causal effects, *arXiv preprint arXiv:2004.14497*.
URL: <https://arxiv.org/abs/2004.14497>
- Kennedy, E. H., Ma, Z., McHugh, M. D. and Small, D. S. (2017). Non-parametric methods for doubly robust estimation of continuous treatment effects, *Journal of the Royal Statistical Society: Series B (Statistical Methodology)* **79**: 1229–1245.
- Kim, B., Khanna, R. and Koyejo, O. O. (2016). Examples are not enough, learn to criticize! criticism for interpretability, *Advances in Neural Information Processing Systems*, pp. 2280–2288.
- Kloog, I., Ridgway, B., Koutrakis, P., Coull, B. A. and Schwartz, J. D. (2013). Long-and short-term exposure to pm2. 5 and mortality: using novel exposure models, *Epidemiology (Cambridge, Mass.)* **24**(4): 555.
- Kuhn, M., Johnson, K. et al. (2013). *Applied predictive modeling*, Vol. 26, Springer.
- Künzel, S. R., Sekhon, J. S., Bickel, P. J. and Yu, B. (2019). Metalearners for estimating heterogeneous treatment effects using machine learning, *Proceedings of the National Academy of Sciences* **116**(10): 4156–4165.
- Lakkaraju, H., Bach, S. H. and Leskovec, J. (2016). Interpretable decision sets: A joint framework for description and prediction, *Proceedings of the 22nd ACM SIGKDD International Conference on Knowledge Discovery and Data Mining*, pp. 1675–1684.
- Lee, K., Small, D. S. and Dominici, F. (2021). Discovering heterogeneous exposure effects using randomization inference in air pollution studies, *Journal of the American Statistical Association* pp. 1–33.
- Lee, M.-j. (2009). Non-parametric tests for distributional treatment effect for randomly censored responses, *Journal of the Royal Statistical Society: Series B (Statistical Methodology)* **71**(1): 243–264.
- Lewis, J. B. and Linzer, D. A. (2005). Estimating regression models in which the dependent variable is based on estimates, *Political Analysis* **13**(4): 345–364.
- Liu, M., Saari, R. K., Zhou, G., Li, J., Han, L. and Liu, X. (2021). Recent trends in premature mortality and health disparities attributable to ambient PM2.5 exposure in China: 2005–2017, *Environmental Pollution* **279**: 116882.
- Loh, W.-Y., Cao, L. and Zhou, P. (2019). Subgroup identification for precision medicine: A comparative review of 13 methods, *Wiley Interdisciplinary Reviews: Data Mining and Knowledge Discovery* **9**(5): e1326.
- Long, J. S. and Ervin, L. H. (2000). Using heteroscedasticity consistent standard errors in the linear regression model, *The American Statistician* **54**(3): 217–224.

- Mayeda, E. R., Filshtein, T. J., Tripodis, Y., Glymour, M. M. and Gross, A. L. (2018). Does selective survival before study enrolment attenuate estimated effects of education on rate of cognitive decline in older adults? A simulation approach for quantifying survival bias in life course epidemiology, *International Journal of Epidemiology* **47**(5): 1507–1517.
- Meinshausen, N. and Bühlmann, P. (2010). Stability selection, *Journal of the Royal Statistical Society: Series B (Statistical Methodology)* **72**(4): 417–473.
- Miller, T. (2019). Explanation in artificial intelligence: Insights from the social sciences, *Artificial Intelligence* **267**: 1–38.
- Nagpal, C., Wei, D., Vinzamuri, B., Shekhar, M., Berger, S. E., Das, S. and Varshney, K. R. (2020). Interpretable subgroup discovery in treatment effect estimation with application to opioid prescribing guidelines, *Proceedings of the ACM Conference on Health, Inference, and Learning*, pp. 19–29.
- Nalenz, M. and Villani, M. (2018). Tree ensembles with rule structured horseshoe regularization, *The Annals of Applied Statistics* **12**(4): 2379–2408.
- Nethery, R. C., Mealli, F., Sacks, J. D. and Dominici, F. (2020). Evaluation of the health impacts of the 1990 clean air act amendments using causal inference and machine learning, *Journal of the American Statistical Association* pp. 1–12.
- Nie, X. and Wager, S. (2017). Quasi-oracle estimation of heterogeneous treatment effects, *Biometrika* **108**: 299–319.
URL: <https://arxiv.org/abs/1712.04912v4>
- Pope III, C. A., Lefler, J. S., Ezzati, M., Higbee, J. D., Marshall, J. D., Kim, S.-Y., Bechle, M., Gilliat, K. S., Vernon, S. E., Robinson, A. L. et al. (2019). Mortality risk and fine particulate air pollution in a large, representative cohort of us adults, *Environmental Health Perspectives* **127**(7): 077007.
- Qian, M. and Murphy, S. A. (2011). Performance guarantees for individualized treatment rules, *Annals of Statistics* **39**(2): 1180.
- Robins, J. M. and Ritov, Y. (1997). Toward a curse of dimensionality appropriate (coda) asymptotic theory for semi-parametric models, *Statistics in medicine* **16**(3): 285–319.
- Robins, J. M., Rotnitzky, A. and Zhao, L. P. (1994). Estimation of regression coefficients when some regressors are not always observed, *Journal of the American statistical Association* **89**(427): 846–866.
- Rosenbaum, P. R. and Rubin, D. B. (1983). The central role of the propensity score in observational studies for causal effects, *Biometrika* **70**(1): 41–55.
- Rubin, D. B. (1974). Estimating causal effects of treatments in randomized and nonrandomized studies., *Journal of Educational Psychology* **66**(5): 688–701.
- Rubin, D. B. (1986). Comment: Which ifs have causal answers, *Journal of the American Statistical Association* **81**(396): 961–962.

- Schwartz, J., Wei, Y., Di, Q., Dominici, F., Zanobetti, A. et al. (2021). A national difference in differences analysis of the effect of pm2. 5 on annual death rates, *Environmental Research* **194**: 110649.
- Semenova, V. and Chernozhukov, V. (2021). Debiased machine learning of conditional average treatment effects and other causal functions, *The Econometrics Journal* **24**(2): 264–289.
- Shaw, C., Hayes-Larson, E., Glymour, M. M., Dufouil, C., Hohman, T. J., Whitmer, R. A., Kobayashi, L. C., Brookmeyer, R. and Mayeda, E. R. (2021). Evaluation of selective survival and sex/gender differences in dementia incidence using a simulation model, *JAMA Network Open* **4**(3): e211001–e211001.
- Spanbauer, C. and Sparapani, R. (2021). Nonparametric machine learning for precision medicine with longitudinal clinical trials and bayesian additive regression trees with mixed models, *Statistics in Medicine* **40**(11): 2665–2691.
- Stone, M. (1974). Cross-validators choice and assessment of statistical predictions, *Journal of the Royal Statistical Society: Series B (Methodological)* **36**(2): 111–133.
- Su, L., Shi, Z. and Phillips, P. C. (2016). Identifying latent structures in panel data, *Econometrica* **84**(6): 2215–2264.
- Tibshirani, R. (1996). Regression shrinkage and selection via the lasso, *Journal of the Royal Statistical Society: Series B (Statistical Methodology)* **58**(1): 267–288.
- U.S. Environmental Protection Agency (2022a). Reconsideration of the national ambient air quality standards for particulate matter, *Technical Report: EPA-452/P-22-001* .
- U.S. Environmental Protection Agency (2022b). Regulatory impact analysis for the proposed reconsideration of the national ambient air quality standards for particulate matter, *Technical Report: EPA-452/P-22-001* .
- Wager, S. and Athey, S. (2018). Estimation and inference of heterogeneous treatment effects using random forests, *Journal of the American Statistical Association* **113**(523): 1228–1242.
- Wang, T. and Rudin, C. (2022). Causal rule sets for identifying subgroups with enhanced treatment effects, *INFORMS Journal on Computing* .
- White, H. (1980). A heteroskedasticity-consistent covariance matrix estimator and a direct test for heteroskedasticity, *Econometrica* **48**(4): 817–838.
- Wu, X., Braun, D., Schwartz, J., Kioumourtzoglou, M. and Dominici, F. (2020). Evaluating the impact of long-term exposure to fine particulate matter on mortality among the elderly, *Science Advances* **6**(29): eaba5692.
- Wu, X., Netherly, R., Sabath, M., Braun, D. and Dominici, F. (2020). Air pollution and covid-19 mortality in the united states: Strengths and limitations of an ecological regression analysis, *Science advances* **6**(45): eabd4049.

- Yang, J., Dahabreh, I. J. and Steingrimsson, J. A. (2021). Causal interaction trees: Finding subgroups with heterogeneous treatment effects in observational data, *Biometrics* .
URL: <http://dx.doi.org/10.1111/biom.13432>
- Yu, B. (2013). Stability, *Bernoulli* **19**(4): 1484–1500.
- Zanobetti, A., Franklin, M., Koutrakis, P. and Schwartz, J. (2009). Fine particulate air pollution and its components in association with cause-specific emergency admissions, *Environmental Health* **8**(1): 1–12.
- Zorzetto, D., Bargagli-Stoffi, F. J., Canale, A. and Dominici, F. (2023). Confounder-dependent bayesian mixture model: Characterizing heterogeneity of causal effects in air pollution epidemiology, *arXiv preprint arXiv:2302.11656* .

SUPPLEMENTARY MATERIAL

A Individual Treatment Effect Estimation

We provide here a brief overview of six of the most successful ITE estimators, highlighting and comparing their strengths and weaknesses. An empirical comparison among these methods is reported in section 4.

A.1 T-Learner

The T-Learner (Hansotia and Rukstales; 2002) is a two-step approach where the conditional mean functions:

$$\mu_0(\mathbf{x}) := \mathbb{E}_i[Y_i(0)|\mathbf{X}_i = \mathbf{x}] \tag{A.1}$$

$$\mu_1(\mathbf{x}) := \mathbb{E}_i[Y_i(1)|\mathbf{X}_i = \mathbf{x}] \tag{A.2}$$

are estimated separately with any supervised learning algorithm (e.g., Generalized Linear Model, Tree Ensemble, Neural Network).

In the first step, the conditional mean under control is estimated by all the observations in the control group ($\hat{\mu}_0(\mathbf{x})$), and the conditional mean under treatment is estimated by all the observations in the treated group ($\hat{\mu}_1(\mathbf{x})$). Then, exploiting equation (2.2), the Treatment Effect is estimated by:

$$\hat{\tau}(\mathbf{x}) = \hat{\mu}_1(\mathbf{x}) - \hat{\mu}_0(\mathbf{x}) \tag{A.3}$$

A.2 S-Learner

The S-learner (Hill; 2011) treats the treatment variable Z_i as if it was just another covariate like those in the vector \mathbf{X}_i . Instead of having two models for the response as a function of the covariates, the S-learner has a single model for the response as a function of the covariates and the treatment:

$$\mu(\mathbf{x}, z) := \mathbb{E}_i[Y_i|\mathbf{X}_i = \mathbf{x}, Z_i = z] \tag{A.4}$$

In the first step, all the observations are used to estimate the response function above, $\hat{\mu}(\mathbf{x}, z)$, by any supervised learning algorithm (e.g., Generalized Linear Model, Tree Ensemble, Neural Network). Then, exploiting equation (2.2), the Treatment Effect is estimated by:

$$\hat{\tau}(\mathbf{x}) = \hat{\mu}(\mathbf{x}, 1) - \hat{\mu}(\mathbf{x}, 0) \quad (\text{A.5})$$

A.3 X-Learner

The X-learner (Künzel et al.; 2019) is a three steps approach, estimating a treatment effect separately for the control and the treatment group. In the first step, like in S-Learner, the conditional mean functions:

$$\mu_0(\mathbf{x}) := \mathbb{E}_i[Y_i(0)|\mathbf{X}_i = \mathbf{x}] \quad (\text{A.6})$$

$$\mu_1(\mathbf{x}) := \mathbb{E}_i[Y_i(1)|\mathbf{X}_i = \mathbf{x}] \quad (\text{A.7})$$

are estimated separately by any supervised learning algorithm (e.g., Generalized Linear Model, Tree Ensemble, Neural Network).

The conditional mean under control is estimated by all the observations in the control group ($\hat{\mu}_0(\mathbf{x})$), and the conditional mean under treatment is estimated by all the observations in the treated group ($\hat{\mu}_1(\mathbf{x})$). Secondly, these two estimates are used for predicting the counterfactual outcomes.

$$\hat{\Psi}_1(\mathbf{X}_i) = Y_i - \hat{\mu}_0(\mathbf{X}_i) \quad \text{for } i : Z_i = 1, \quad (\text{A.8})$$

$$\hat{\Psi}_0(\mathbf{X}_i) = \hat{\mu}_1(\mathbf{X}_i) - Y_i \quad \text{for } i : Z_i = 0. \quad (\text{A.9})$$

Finally, these imputed effects are regressed individually on the covariates to obtain $\hat{\tau}_0(\mathbf{x})$ (the CATE for the control group) and $\hat{\tau}_1(\mathbf{x})$ (the CATE for the treatment group), and then combined by a weight function $g \in [0, 1]$:

$$\hat{\tau}(\mathbf{x}) = g(\mathbf{x})\hat{\tau}_0(\mathbf{x}) + [1 - g(\mathbf{x})]\hat{\tau}_1(\mathbf{x}) \quad (\text{A.10})$$

A good choice for g is an estimate of the propensity score.

A.4 Augmented Inverse Probability Weighting (AIPW)

The Augmented Inverse Probability Weighting estimator (Robins et al.; 1994; Robins and Ritov; 1997) extends the observations balancing of Inverse Probability Weighting methods (Horvitz and Thompson; 1952) with conditional response estimation of the S-Learner, inheriting the benefits of both the approaches.

Firstly, the conditional mean response:

$$\mu(\mathbf{x}, z) := \mathbb{E}_i[Y_i | \mathbf{X}_i = \mathbf{x}, Z_i = z] \tag{A.11}$$

is estimated from all the observations by any supervised learning algorithm, $\hat{\mu}(\mathbf{x}, z)$ (first step S-Learner). Then, the propensity score:

$$e(\mathbf{x}) := \mathbb{E}_i[Z_i | \mathbf{X}_i = \mathbf{x}] \tag{A.12}$$

is estimated from all the observations by any supervised learning algorithm, $\hat{e}(\mathbf{x})$.

Finally, the Treatment Effect is computed by:

$$\hat{\tau}(\mathbf{x}) = \frac{1}{N} \sum_{i \in \mathcal{I}(\mathbf{x})} \left\{ \left(\hat{\mu}(\mathbf{X}_i, 1) + \frac{Z_i(Y_i - \hat{\mu}(\mathbf{X}_i, 1))}{\hat{e}(\mathbf{X}_i)} \right) - \left(\hat{\mu}(\mathbf{X}_i, 0) + \frac{(1 - Z_i)(Y_i - \hat{\mu}(\mathbf{X}_i, 0))}{1 - \hat{e}(\mathbf{X}_i)} \right) \right\} \tag{A.13}$$

where $\mathcal{I}(\mathbf{x}) = \{i \in \mathcal{I} : \mathbf{X}_i = \mathbf{x}\}$. By construction, it is only required that one estimator among \hat{e} and $\hat{\mu}$ is unbiased in order to get an unbiased estimate of the treatment effect.

A.5 Causal Bayesian Additive Regression Trees (Causal BART)

The Bayesian Additive Regression Trees (BART) approach (Chipman et al.; 2010) combines gradient-boosting trees in a Bayesian framing using Markov Chain Monte Carlo (MCMC) sampling for back fitting (using additive and generalized additive models for posterior sampling). The

Causal Bayesian Additive Regression Trees (Causal BART) approach (Hill; 2011) relies on such non-parametric Bayesian models to estimate treatment effects via S-Learner (see equation (A.5)). The method is specially designed to estimate the Treatment Effect from observational studies with small effect sizes and heterogeneous effects.

A.6 Bayesian Causal Forest (BCF)

The Bayesian Causal Forest (Hahn et al.; 2020) is a state-of-the-art model for causal inference that builds on Bayesian Additive Regression Trees. BCF combines Bayesian regularization with regression trees to provide a highly flexible response surface that, thanks to regularization from prior distributions, does not overfit the training data. In particular, BCF model the response as a function of the covariates and the treatment, adding the following priors:

$$\mu(\mathbf{x}, z) := \mathbb{E}_i[Y_i | \mathbf{X}_i = \mathbf{x}, Z_i = z] \tag{A.14}$$

$$= \mu(\mathbf{x}, \hat{e}(z)) + \tau(\mathbf{x})z \tag{A.15}$$

where $\hat{e}(\mathbf{x})$ is the estimated propensity score and the functions $\mu(\mathbf{x})$ and $\tau(\mathbf{x})$ are independent BART priors. The inclusion of the estimated propensity score can be seen as a covariate-dependent prior to controlling for confounding bias. The treatment effect is then computed as a S-Learner estimator by equation (A.5).

B Filtering

In the discovery step, once a set of candidate decision rules ($\hat{\mathcal{R}}''$) has been proposed, we discard all the extreme or redundant decision rules based on the following two criteria:

- i. **Extreme:** A (candidate) decision rule $r_m \in \hat{\mathcal{R}}''$ is said extreme if either too rare:

$$\sum_{i \in \mathcal{I}^{dis}} r_m(\mathbf{X}_i) \leq t_{ext} N^{dis}, \tag{B.1}$$

or too common:

$$\sum_{i \in \mathcal{I}^{dis}} r_m(\mathbf{X}_i) \geq (1 - t_{ext})N^{dis}, \quad (\text{B.2})$$

where t_{ext} is the threshold parameter defining the limit ratio, and $N^{dis} = |\mathcal{I}^{dis}|$.

- ii. **Redundant:** A (candidate) decision rule $r_a \in \hat{\mathcal{R}}''$ is said redundant if exists at least another (candidate) decision rule $r_b \in \hat{\mathcal{R}}''$ such that their correlation is greater than a fixed threshold (t_{corr}).

These filtering criteria help in practice to preliminary filter irrelevant decision rules and speed up the rules selection step.

C Mathematical Proofs

In this Appendix, we report the proofs of the Propositions presented in section 3.

C.1 Proposition 1. (Consistency of the AATE estimator)

Proposition 1. *Let $\hat{\tau}$ a consistent estimator for τ (i.e., AIPW). Under the Treatment Effect linear decomposition Assumption (Condition 1) and assuming $\mathbb{E}(\mathbf{R}^T \mathbf{R}) = \mathbf{Q}$ is a positive definite matrix (Condition 2), the Additive Average Treatment Effects estimator $\hat{\alpha} = (\mathbf{R}^T \mathbf{R})^{-1} \mathbf{R}^T (\hat{\tau} - \hat{\tau})$ is a consistent estimator for α .*

Proof. Multiplying equation (2.8) (Condition 1) on the both sides by $(\mathbf{R}^T \mathbf{R})^{-1} \mathbf{R}^T$, we get:

$$(\mathbf{R}^T \mathbf{R})^{-1} \mathbf{R}^T (\hat{\tau} - \hat{\tau}) = (\mathbf{R}^T \mathbf{R})^{-1} \mathbf{R}^T \mathbf{R} \alpha + (\mathbf{R}^T \mathbf{R})^{-1} \mathbf{R}^T \boldsymbol{\nu}. \quad (\text{C.1})$$

Using equation (3.7), and simplifying the right member:

$$\rightarrow \hat{\alpha} = \alpha + (\mathbf{R}^T \mathbf{R})^{-1} \mathbf{R}^T \boldsymbol{\nu}. \quad (\text{C.2})$$

Observing that by Condition 2 and the Law of large numbers:

$$\frac{R^T R}{N} = \frac{1}{N} \sum_{i=1}^N \mathbf{R}_i^T \cdot \mathbf{R}_i \xrightarrow{d} Q \succ 0, \quad (\text{C.3})$$

where \mathbf{R}_i represents the i -th row of the rules matrix, and:

$$\frac{R^T \boldsymbol{\nu}}{N} = \frac{1}{N} \sum_{i=1}^N \mathbf{R}_i^T \cdot \nu_i \xrightarrow{d} \mathbf{0}; \quad (\text{C.4})$$

combining them in equation (C.2) (simplifying N), by Slutsky's theorem:

$$\hat{\boldsymbol{\alpha}} \xrightarrow{d} \boldsymbol{\alpha} \quad (\text{C.5})$$

□

C.1.1 Proposition 2. (Asymptotic Normality of the AATE estimator)

Proposition 2. *If Conditions (1)-(5) hold, then*

$$\sqrt{N}(\hat{\boldsymbol{\alpha}} - \boldsymbol{\alpha}) \xrightarrow{d} \mathcal{N}(0, V) \text{ as } N \rightarrow \infty \quad (\text{C.6})$$

where $V = Q^{-1}\Omega Q^{-1}$.

Proof. Similarly to the proof of Proposition (1), multiplying equation (2.8) (Condition 1) on the both sides by $(R^T R)^{-1} R^T$, and inserting equation (3.7), we get:

$$\hat{\boldsymbol{\alpha}} = \boldsymbol{\alpha} + (R^T R)^{-1} R^T \boldsymbol{\nu}. \quad (\text{C.7})$$

Multiplying both sides by \sqrt{N} and rearranging we get:

$$\begin{aligned} \sqrt{N}(\hat{\boldsymbol{\alpha}} - \boldsymbol{\alpha}) &= \left(\frac{R^T R}{N} \right)^{-1} \frac{R^T \boldsymbol{\nu}}{\sqrt{N}} \\ &= \left(\frac{\sum_{i=1}^N \mathbf{R}_i^T \mathbf{R}_i}{N} \right)^{-1} \frac{\sum_{i=1}^N \mathbf{R}_i^T \nu_i}{\sqrt{N}} \end{aligned}$$

By hypothesis:

$$\mathbb{E}[\mathbf{R}_i \nu_i] = \mathbf{0} \quad \forall i \in \mathcal{I}^e \quad (\text{C.8})$$

and:

$$\begin{aligned} \text{Var}(\mathbf{R}_i \nu_i) &= \mathbb{E}[\nu_i^2 \mathbf{R}_i^T \mathbf{R}_i] - \mathbb{E}[\mathbf{R}_i \nu_i]^2 \\ \& &= \mathbb{E}[\nu_i^2 \mathbf{R}_i^T \mathbf{R}_i] = \Omega \succ 0 \quad \forall i \in \mathcal{I}^e \end{aligned} \quad (\text{C.9})$$

Then, by the Central Limit Theorem:

$$\frac{\sum_{i=1}^N \mathbf{R}_i^T \nu_i}{N} \xrightarrow{d} \mathcal{N}(0, \Omega). \quad (\text{C.10})$$

We have already discussed in the proof of Proposition (1) that:

$$\frac{R^T R}{N} = \frac{1}{N} \sum_{i=1}^N \mathbf{R}_i^T \cdot \mathbf{R}_i \xrightarrow{d} Q \succ 0. \quad (\text{C.11})$$

Then, combining these results in equation (C.8), by Slutsky' theorem and Cramer-Wold theorem:

$$\sqrt{N}(\hat{\boldsymbol{\alpha}} - \boldsymbol{\alpha}) \xrightarrow{d} \mathcal{N}(0, Q^{-1} \Omega Q^{-1}) \quad \text{as } N \rightarrow \infty \quad (\text{C.12})$$

□

D Additional Simulations

In this Appendix, we present a more extensive analysis of the heterogeneity discovery and treatment effect estimation simulation studies under different variants of the data-generating process, varying the sample size, the number of decision rules, the complexity of the decision rules, and the type of confounding. In particular, for both the simulation studies, we consider the following five variants to the data generating process described in Section 4 (where all the definitions are kept equal if not otherwise specified):

- i. **Large Sample:** $N = 5,000$ individuals, $M = 2$ rules (r_1, r_2) , linear confounding;

ii. **Small Sample:** $N = 1,000$ individuals, $M = 2$ rules (r_1, r_2), linear confounding;

iii. **More Rules:** $N = 2,000$ individuals, $M = 4$ rules (r_1, r_2, r_3, r_4), linear confounding, where:

$$\begin{aligned}\mu_i^0 &= X_i^1 + X_i^3 + X_i^4 + k \cdot \mathbb{1}_{\{x_1=1;x_2=0\}}(\mathbf{X}_i) + \frac{k}{2} \cdot \mathbb{1}_{\{x_4=0\}}(\mathbf{X}_i) \\ &= X_i^1 + X_i^3 + X_i^4 + k \cdot r_1(\mathbf{X}_i) + \frac{k}{2} \cdot r_3(\mathbf{X}_i),\end{aligned}$$

$$\begin{aligned}\mu_i^1 &= X_i^1 + X_i^3 + X_i^4 + k \cdot \mathbb{1}_{\{x_5=1;x_6=0\}}(\mathbf{X}_i) + 2k \cdot \mathbb{1}_{\{x_5=0;x_7=1;x_8=0\}}(\mathbf{X}_i) \\ &= X_i^1 + X_i^3 + X_i^4 + k \cdot r_2(\mathbf{X}_i) + 2k \cdot r_4(\mathbf{X}_i),\end{aligned}$$

and then:

$$\tau(\mathbf{x}) = -k \cdot r_1(\mathbf{x}) + k \cdot r_2(\mathbf{x}) - \frac{k}{2} \cdot r_3(\mathbf{x}) + 2k \cdot r_4(\mathbf{x});$$

iv. (Pseudo) **Randomized Controlled Trial:** $N = 2,000$ individuals, $M = 2$ rules (r_1, r_2), only confounding by decision rules, i.e.:

$$\begin{aligned}\mu_i^0 &= k \cdot \mathbb{1}_{\{x_1=1;x_2=0\}}(\mathbf{X}_i) = k \cdot r_1(\mathbf{X}_i), \\ \mu_i^1 &= k \cdot \mathbb{1}_{\{x_5=1;x_6=0\}}(\mathbf{X}_i) = k \cdot r_2(\mathbf{X}_i);\end{aligned}$$

and then (as the original data-generating process):

$$\tau(\mathbf{x}) = -k \cdot r_1(\mathbf{x}) + k \cdot r_2(\mathbf{x});$$

v. **Non-Linear Confounding:** $N = 2,000$ individuals, $M = 2$ rules (r_1, r_2), non-linear confounding, i.e.:

$$\begin{aligned}\mu_i^0 &= X_i^1 + \sin(x_i^3 \cdot x_i^4) + k \cdot \mathbb{1}_{\{x_1=1;x_2=0\}}(\mathbf{X}_i) = k \cdot r_1(\mathbf{X}_i), \\ \mu_i^1 &= X_i^1 + \sin(x_i^3 \cdot x_i^4) + k \cdot \mathbb{1}_{\{x_5=1;x_6=0\}}(\mathbf{X}_i) = k \cdot r_2(\mathbf{X}_i).\end{aligned}$$

and then (as the original data-generating process):

$$\tau(\mathbf{x}) = -k \cdot r_1(\mathbf{x}) + k \cdot r_2(\mathbf{x});$$

Each of the described data-generating processes vary the original design for a specific characteristic, which we desire to test our methodology on. In Section D.1 we report and discuss the results of the heterogeneity discovery simulation study over these different data-generating processes, and in Section D.1 we report and discuss the results of the heterogeneous treatment effect estimation simulation study over the same instances.

D.1 Discovery

In this Section, we discuss, one by one, the results of the simulations study on heterogeneity discovery presented in Section 4.1 on the five variant data-generating processes described above.

D.1.1 Large Sample

In Figure D.1 we report the results for heterogeneity discovery increasing the sample size to $N = 5,000$ individuals. As expected, all the methods follow the same trends described for the original data-generating process, but significantly increase the convergence rate, in particular for the *Recall* in both Estimation and Decision Rules retrieval. CRE (AIPW) is the unique method not speeding up the convergence rate to perfect recovery, probably due to its instability issued already discussed in Section 4.2.

D.1.2 Small Sample

In Figure D.2 we report the results for heterogeneity discovery decreasing the sample size to $N = 1,000$ individuals. As expected, all the methods follow the same trends described for the original data-generating process, without significantly decreasing the convergence rate toward perfect discovery. These results strongly encourage the use of CRE even in a small sample regime.

D.1.3 More Rules

In Figure D.3, we report the results for heterogeneity discovery, increasing the number of decision rules to $M = 4$. As expected, (almost) all the methods increase their discovery performances, increasing the causal effect (k). There are now seven effect modifiers out of $p = 10$ covariates, which leads to easier effect modifiers retrieval. The decision rules discovery is instead more challenging due to the higher and heterogeneous/more complex number of rules to retrieve. All the methods still perfectly retrieve all the true decision rules with $k > 3$ ($Recall = 1$), but again, they often retrieve also wrong or redundant rules ($Precision < 1$).

D.1.4 Randomized Controlled Trial

In Figure D.4, we report the results for heterogeneity discovery with no confounding (if not in terms of decision rules). As expected, all the methods follow the same trends described for the original data-generating process, but significantly and equally increase the convergence rate, in particular for the $Recall$ in both estimation and decision rules retrieval. Indeed, removing additional confounding mechanism facilitate all the estimation steps.

D.1.5 Non-Linear Confounding

In Figure D.5, we report the results for heterogeneity discovery with non-linear confounding. As expected, all the methods follow the same trends described for the original data-generating process, without significantly decreasing the convergence rate towards perfect discovery, although the more complex confounding mechanism.

D.2 Estimation

In this Section, we discuss, one by one, the results of the simulations study on heterogeneous treatment effect estimation presented in Section 4.2 on the five variant data generating processes described above.

D.2.1 Large Sample

In Table D.1, we report the results for heterogeneous treatment effect estimation, increasing the sample size to $N = 5,000$ individuals. As discussed in Section 4.2, all the CRE variants signifi-

Method	RMSE		Bias	
	μ	σ	μ	σ
CRE (AIPW)	0.0804	0.0357	0.0011	0.0527
CRE (BCF)	0.0891	0.0324	0.0022	0.0488
CRE (S-Learner)	0.0918	0.0332	0.0010	0.0497
CRE (T-Learner)	0.0905	0.0343	0.0034	0.0522
CRE (X-Learner)	0.0850	0.0337	0.0034	0.0522
CRE (Causal BART)	0.0781	0.0306	0.0002	0.0490
AIPW	2.2526	0.0910	0.0016	0.0342
BCF	0.0814	0.0234	0.0020	0.0319
S-Learner	0.3110	0.0218	0.0012	0.0333
T-Learner	0.5090	0.0214	0.0024	0.0333
X-Learner	1.0756	0.0140	0.0024	0.0333
Causal BART	0.9977	0.0099	0.0003	0.0315

Table D.1: Simulation study for HTE estimation, with $M = 2$ rules, linear confounder, 5,000 individuals, and under CATE linear decomposition assumption. For all the methods, the mean (μ) and standard deviation (σ) treatment effect root mean squared error (RMSE) and bias (Bias) over 250 Monte Carlo experiments are reported.

cantly outperform the corresponding ‘standalone’ ITE estimators in both ITE and ATE estimation. Bayesian Causal Forest is the unique ITE estimator in getting similar performances to the corresponding CRE variant. AIPW estimator still suffers from not stabilized ITE prediction.

In Figure D.6, we report the results for AATEs estimation, increasing the sample size to $N = 5,000$ individuals. As expected from Proposition 2, all the methods lead to consistent AATEs estimation, with a confidence interval even smaller than the original data-generating process.

D.2.2 Small Sample

In Table D.2, we report the results for heterogeneous treatment effect estimation, decreasing the sample size to $N = 1,000$ individuals. As discussed in Section 4.2, (almost) all the CRE variants significantly outperform the corresponding ‘standalone’ ITE estimators in both ITE and ATE estimation without significantly worsening the performances from the original data-generating process

Method	RMSE		Bias	
	μ	σ	μ	σ
CRE (AIPW)	0.2195	0.0882	-0.0136	0.1343
CRE (BCF)	0.2215	0.0758	0.0055	0.1182
CRE (S-Learner)	0.2312	0.0880	-0.0132	0.1321
CRE (T-Learner)	0.1976	0.0859	-0.0265	0.1194
CRE (X-Learner)	0.1961	0.0854	-0.0265	0.1194
CRE (Causal BART)	0.2225	0.0821	-0.0003	0.1187
AIPW	1.7045	0.1320	-0.0037	0.0843
BCF	0.2056	0.0570	0.0022	0.0847
S-Learner	0.6844	0.0590	-0.0030	0.0808
T-Learner	1.1078	0.0590	-0.0064	0.0858
X-Learner	1.3403	0.0527	-0.0064	0.0858
Causal BART	0.9862	0.0248	-0.0007	0.0850

Table D.2: Simulation study for HTE estimation, with $M = 2$ rules, linear confounder, 1,000 individuals, and under CATE linear decomposition assumption. For all the methods, the mean (μ) and standard deviation (σ) treatment effect root mean squared error (RMSE) and bias (Bias) over 250 Monte Carlo experiments are reported.

(with larger sample size), with exceptions of BCF.

In Figure D.7, we report the results for AATEs estimation, increasing the sample size to $N = 1,000$ individuals. As expected from Proposition 2, all the methods lead to consistent AATEs estimation, with not significantly larger confidence intervals with respect to the original data generating process, although the sample size.

D.2.3 More Rules

In Table D.3, we report the results for heterogeneous treatment effect estimation, increasing the number of decision rules to $M = 4$. As discussed in Section 4.2, (almost) all the CRE variants significantly outperform the corresponding ‘standalone’ ITE estimators in both ITE and ATE estimation without significantly worsening the performances from the original data-generating process (with simpler CATE decomposition), with exceptions of BCF.

In Figure D.8, we report the results for AATEs estimation, increasing the number of decision rules to $M = 4$. As expected from Proposition 2, all the methods lead to consistent AATE estimation for (almost) all the rules. Only the fourth and longest rule is slightly underestimated

Method	RMSE		Bias	
	μ	σ	μ	σ
CRE (AIPW)	0.2505	0.1897	-0.0029	0.0936
CRE (BCF)	0.1901	0.0884	0.0061	0.0804
CRE (S-Learner)	0.2967	0.1394	-0.0044	0.0900
CRE (T-Learner)	0.2349	0.0943	0.0003	0.0944
CRE (X-Learner)	0.2356	0.1416	0.0003	0.0948
CRE (Causal BART)	0.1757	0.0729	-0.0017	0.0810
AIPW	2.1139	0.2077	0.0007	0.0561
BCF	0.1698	0.0353	0.0045	0.0519
S-Learner	0.5410	0.0394	-0.0006	0.0532
T-Learner	0.8075	0.0371	0.0026	0.0567
X-Learner	1.1883	0.0293	0.0026	0.0567
Causal BART	0.9994	0.0161	0.0012	0.0517

Table D.3: Simulation study for HTE estimation, with $M = 4$ rules, linear confounder, 2,000 individuals, and under CATE linear decomposition assumption. For all the methods, the mean (μ) and standard deviation (σ) treatment effect root mean squared error (RMSE) and bias (Bias) over 250 Monte Carlo experiments are reported.

by almost all the methods, probably due to the redundant recovery of other similar decision rules ($Precision < 1$).

D.2.4 Randomized Controlled Trial

In Table D.4, we report the results for heterogeneous treatment effect estimation, with no confounding (if not in terms of decision rules). As discussed in Section 4.2, (almost) all the CRE variants significantly outperform the corresponding ‘standalone’ ITE estimators in both ITE and ATE estimation without significantly worsening the performances from the original data-generating process (with linear confounding), with exceptions of BCF. Given the similarity of the results with the original data-generating process, we empirically observe that the under the assumption of unconfoundness (Assumption 3) CRE algorithm is robust with respect to the confounding mechanism. CRE (AIPW) is the best-performing method in ITE estimation (although the unstable AIPW pseudo-outcome estimation) and CRE (Causal BART) leads to the most consistent estimate.

In Figure D.9, we report the results for AATEs estimation, with no confounding (if not in terms of decision rules). As expected from Proposition 2, all the methods lead to consistent AATEs

Method	RMSE		Bias	
	μ	σ	μ	σ
CRE (AIPW)	0.1342	0.0602	0.0031	0.0884
CRE (BCF)	0.1492	0.0552	0.0047	0.0796
CRE (S-Learner)	0.1465	0.0576	0.0025	0.0848
CRE (T-Learner)	0.1489	0.0659	0.0062	0.0931
CRE (X-Learner)	0.1443	0.0655	0.0062	0.0931
CRE (Causal BART)	0.1457	0.0621	0.0010	0.0810
AIPW	2.0757	0.1897	0.0039	0.0560
BCF	0.1351	0.0371	0.0045	0.0517
S-Learner	0.4690	0.0342	0.0031	0.0527
T-Learner	0.8042	0.0367	0.0042	0.0563
X-Learner	1.1863	0.0286	0.0042	0.0563
Causal BART	0.9924	0.0165	0.0021	0.0523

Table D.4: Simulation study for HTE estimation, with $M = 2$ rules, no-confounder (randomized controlled trial), 2,000 individuals and under CATE linear decomposition assumption. For all the methods, the mean (μ) and standard deviation (σ) treatment effect root mean squared error (RMSE) and bias (Bias) over 250 Monte Carlo experiments are reported.

estimation.

D.2.5 Non-Linear Confounding

In Table D.5, we report the results for heterogeneous treatment effect estimation with non-linear confounding. The confounding mechanism doesn't seem to significantly impact the estimation performances, and the results obtained look very similar to the ones from the original data-generating process and the randomized controlled experiment variant. As discussed in Section 4.2, (almost) all the CRE variants significantly outperform the corresponding 'standalone' ITE estimators in both ITE and ATE estimation without significantly worsening the performances from the original data-generating process (with linear confounding), with exceptions of BCF.

In Figure D.10, we report the results for AATEs estimation, with non-linear confounding. As expected from Proposition 2, all the methods lead to consistent AATEs estimation.

Method	RMSE		Bias	
	μ	σ	μ	σ
CRE (AIPW)	0.1343	0.0601	0.0037	0.0881
CRE (BCF)	0.1493	0.0555	0.0050	0.0790
CRE (S-Learner)	0.1492	0.0599	0.0035	0.0849
CRE (T-Learner)	0.1490	0.0664	0.0074	0.0937
CRE (X-Learner)	0.1460	0.0651	0.0073	0.0938
CRE (Causal BART)	0.1421	0.0628	0.0002	0.0817
AIPW	2.0767	0.1945	0.0043	0.0560
BCF	0.1347	0.0370	0.0045	0.0524
S-Learner	0.4721	0.0333	0.0033	0.0529
T-Learner	0.8052	0.0373	0.0048	0.0568
X-Learner	1.1870	0.0292	0.0048	0.0568
Causal BART	0.9925	0.0164	0.0019	0.0517

Table D.5: Simulation study for HTE estimation, with $M = 2$ rules, non-linear confounder, 2,000 individuals, and under CATE linear decomposition assumption. For all the methods, the mean (μ) and standard deviation (σ) treatment effect root mean squared error (RMSE) and bias (Bias) over 250 Monte Carlo experiments are reported.

E Parameter Settings

In this section, we summarize the parameter settings. In Table E.1, we report the default CRE method and hyperparameters used for the simulation studies. In Table E.2, we report the default CRE method and hyperparameters used for the applied experiment on the discovery and estimation of HTE of air pollution exposure on mortality. In both the tables, ‘XGboost’ stands for the scalable end-to-end tree-boosting system algorithm by [Chen and Guestrin \(2016\)](#).

	Parameter	Value
Honest Splitting	Ratio	0.5
Discovery		
ITE Estimation	Propensity Score estimator (\hat{e})	XGboost
	Outcome estimator ($\hat{\mu}$)	XGBoost
Rules Generation	N. Trees (Random Forest)	40
	N. Trees (GBM)	40
	Replace	True
	Max node (subgroup) size	20
	Max depth (L)	3
	Max number of nodes (per tree)	$2^3 = 8$
Filtering	t_{decay}	0.025
	t_{ext}	0.01
	t_{corr}	1
Rules Selection	Upper Bound PFER	$\frac{L}{k+1}$
	π_{thr}	0.8
Estimation		
ITE Estimation	Propensity Score estimator (\hat{e})	XGboost
	Outcome estimator ($\hat{\mu}$)	XGBoost
CATE Estimation	$t_{p\text{-value}}$	0.05

Table E.1: List of CRE method parameters and hyperparameters used for the simulations.

	Parameter	Value
Honest Splitting	Ratio	0.5
Discovery		
ITE Estimation	Estimator	X-Learner
	Outcome estimator ($\hat{\mu}$)	XGBoost
Rules Generation	N. Trees (Random Forest)	100
	N. Trees (GBM)	100
	Replace	True
	Max node (subgroup) size	20
	Max depth (L)	2
	Max number of nodes (per tree)	4
Filtering	t_{decay}	0.002
	t_{ext}	0.005
	t_{corr}	1
Rules Selection	Upper Bound PFER	1
	π_{thr}	0.8
Estimation		
ITE Estimation	Estimator	X-Learner
	Outcome estimator ($\hat{\mu}$)	XGBoost
CATE Estimation	$t_{p\text{-value}}$	0.05

Table E.2: List of CRE method parameters and hyper-parameters used for the discovery and estimation of HTE of air pollution exposure on mortality.

F Additional Figures

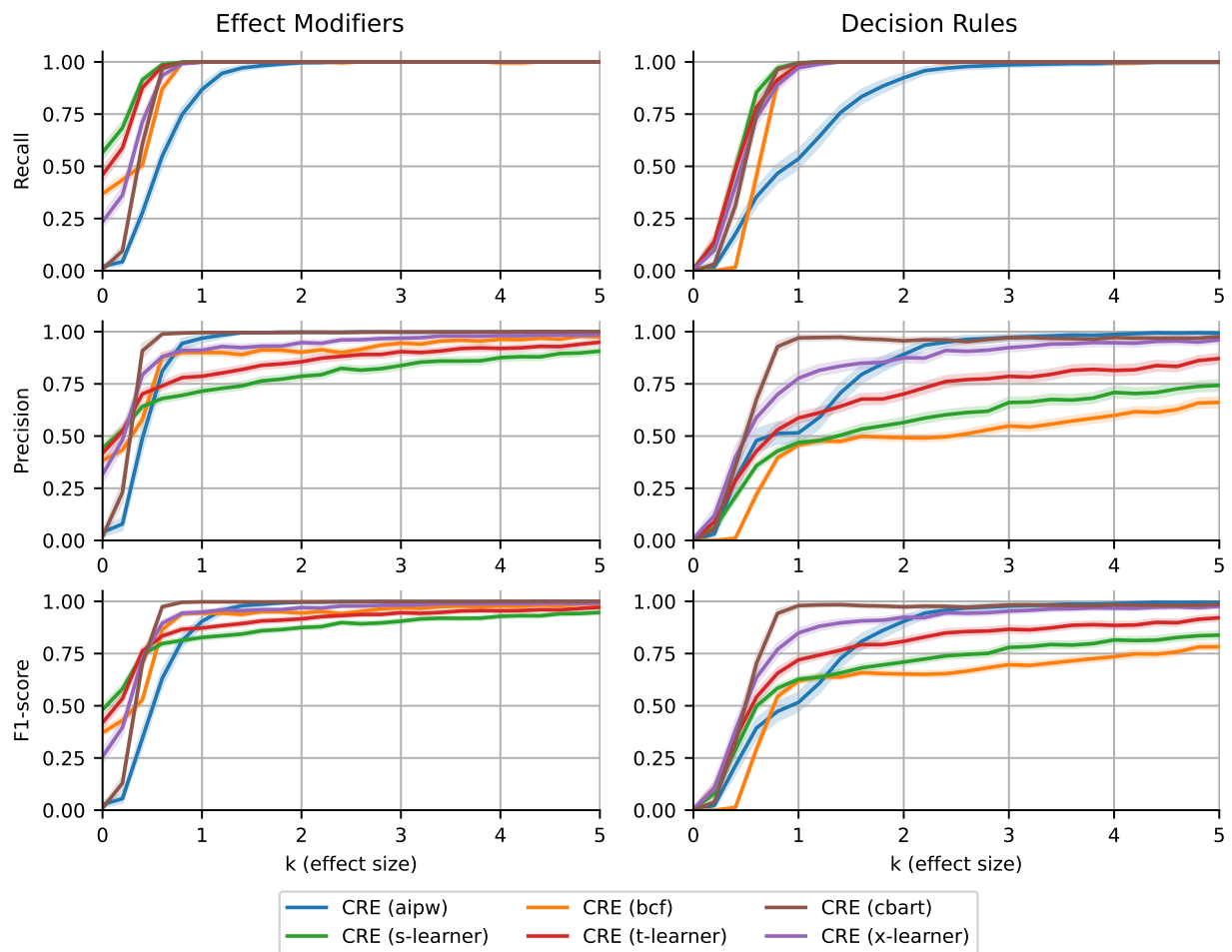


Figure D.1: Simulation study for heterogeneity discovery results with 2 rules, linear confounders and 5,000 observations. Mean *Precision*, *Recall* and *F1-score* (lines) with the corresponding 95% confidence intervals (bands) over 250 Monte Carlo experiments are reported for each method and causal effect size k . For each CRE variant, the heterogeneity characterization discovery converges (with respect to effect size) to the true heterogeneity characterization.

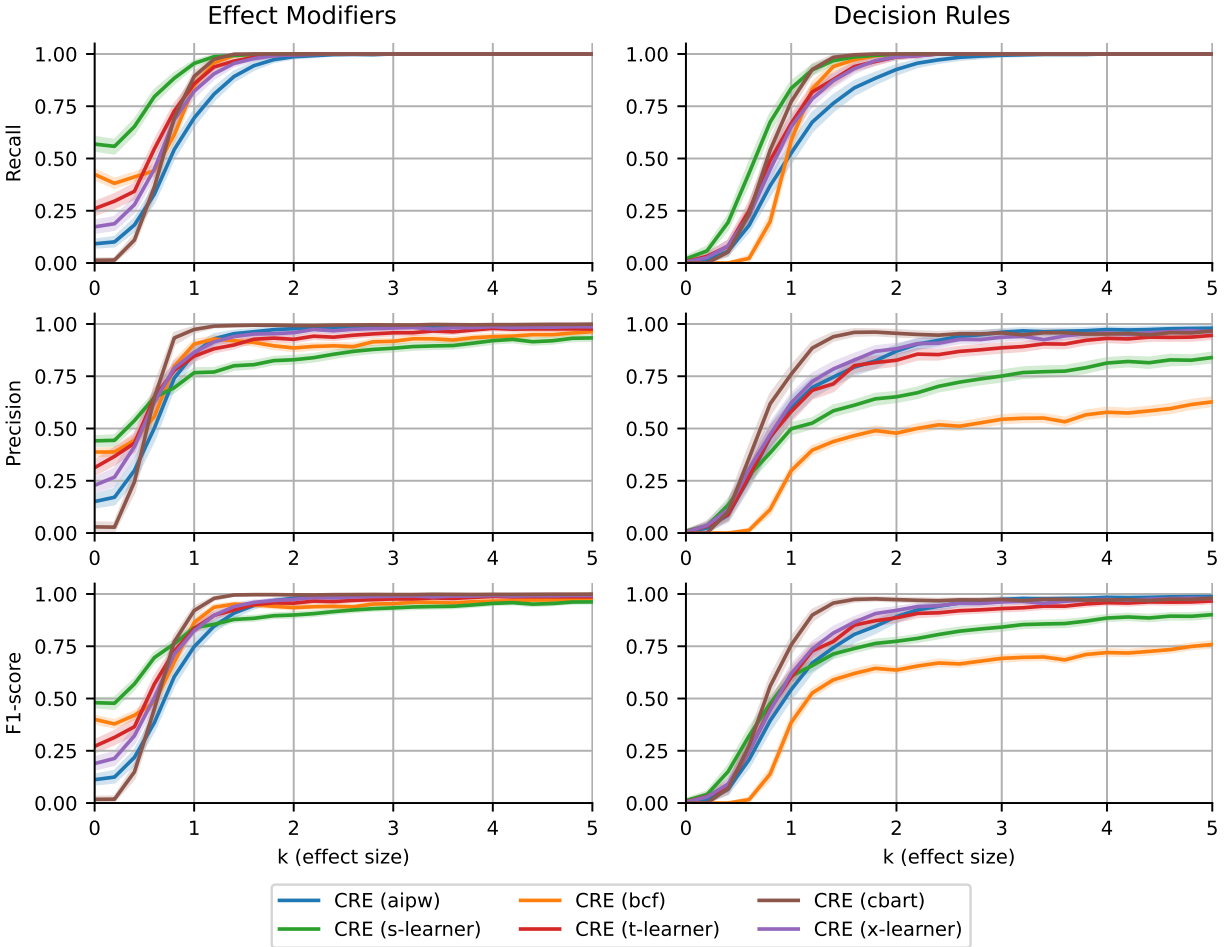


Figure D.2: Simulation study for heterogeneity discovery results with 2 rules, linear confounders, and 1,000 observations. Mean *Precision*, *Recall*, and *F1-score* (lines) with the corresponding 95% confidence intervals (bands) over 250 Monte Carlo experiments are reported for each method and causal effect size k . For each CRE variant, the heterogeneity characterization discovery converges (with respect to effect size) to the true heterogeneity characterization.

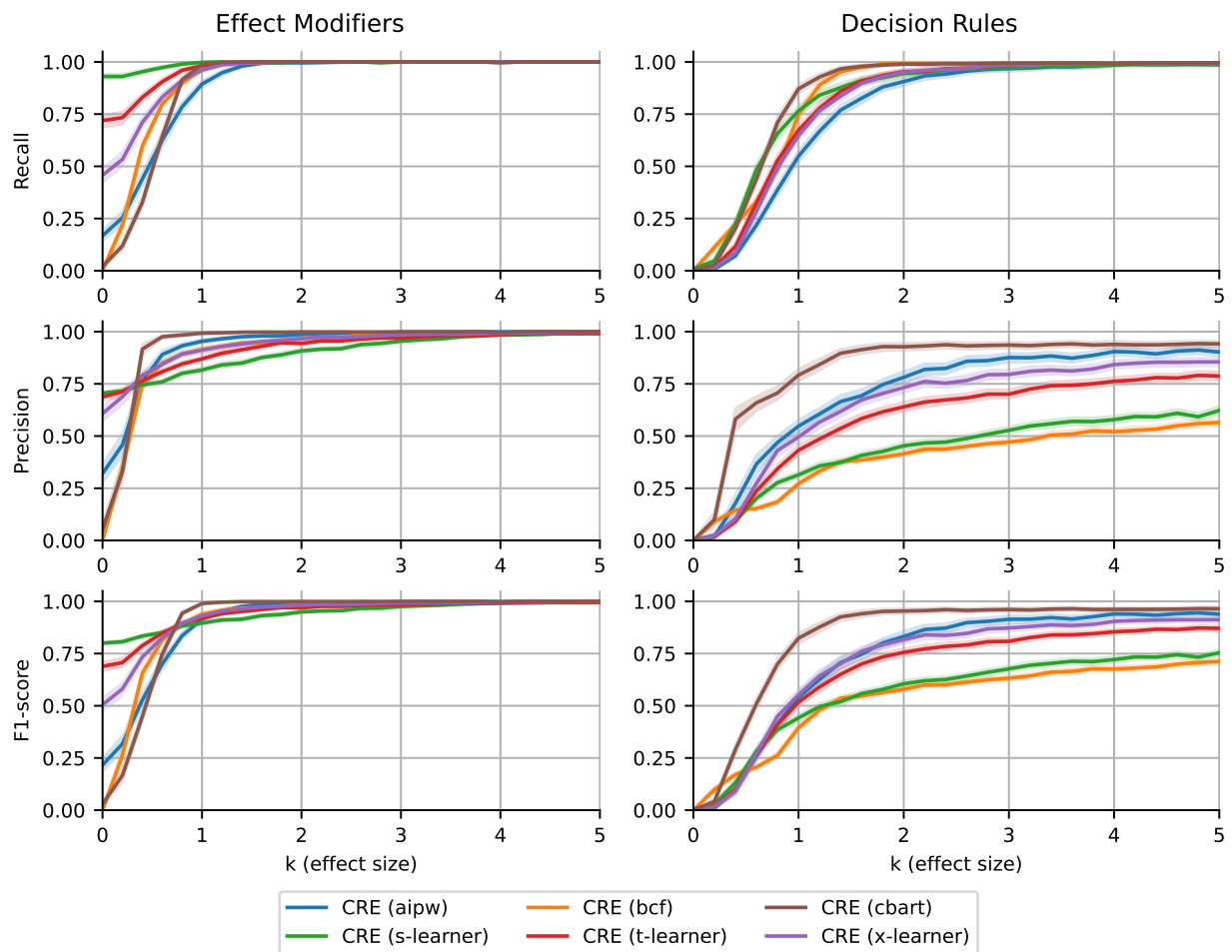


Figure D.3: Simulation study for heterogeneity discovery results with 4 rules, linear confounders, and 2,000 observations. Mean *Precision*, *Recall* and *F1-score* (lines) with the corresponding 95% confidence intervals (bands) over 250 Monte Carlo experiments are reported for each method and causal effect size k . For each CRE variant, the heterogeneity characterization discovery converges (with respect to effect size) to the true heterogeneity characterization.

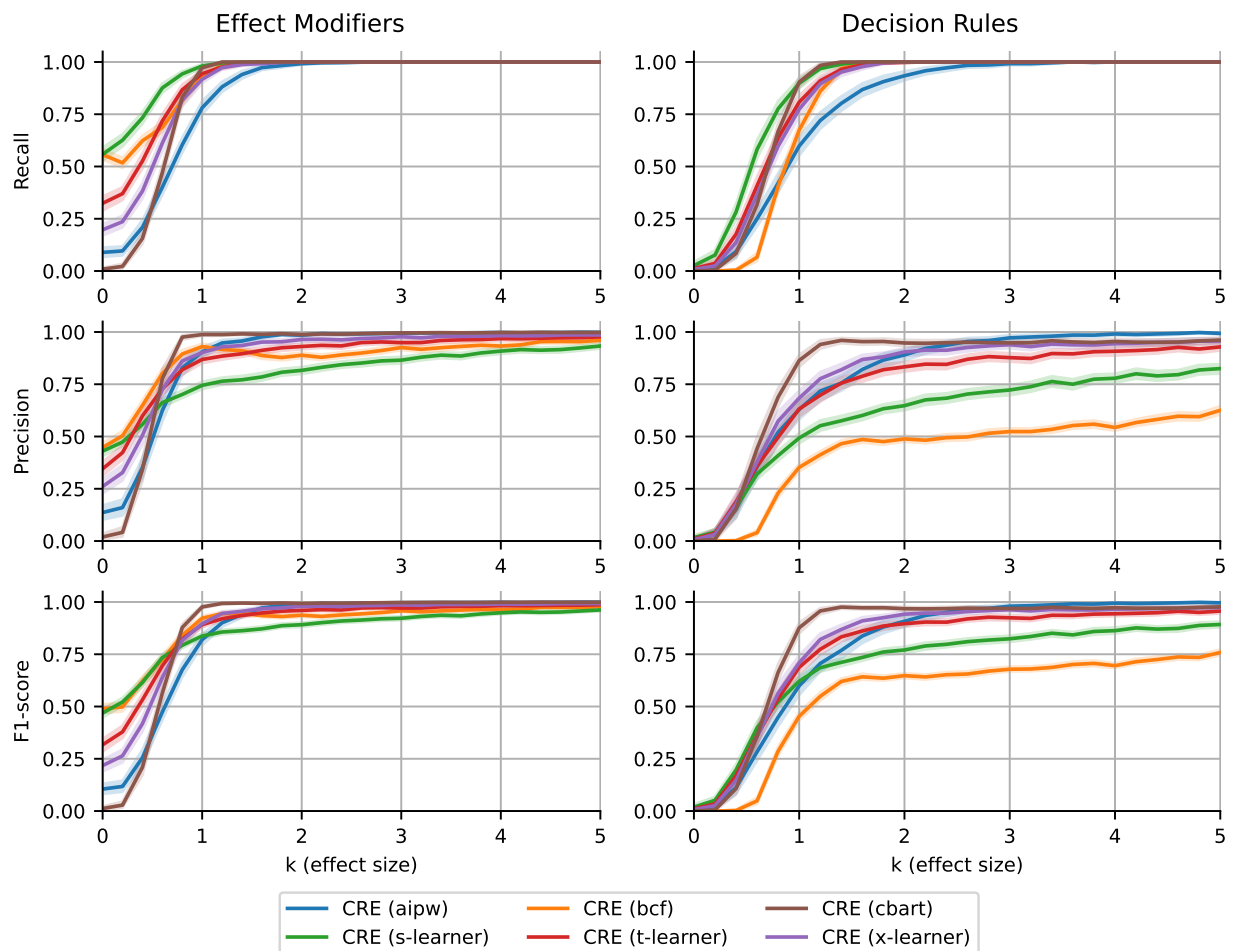


Figure D.4: Simulation study for heterogeneity discovery results with 2 rules, no confounders (randomized controlled trial), and 2,000 observations. Mean *Precision*, *Recall*, and *F1 – score* (lines) with the corresponding 95% confidence intervals (bands) over 250 Monte Carlo experiments are reported for each method and causal effect size k . For each CRE variant, the heterogeneity characterization discovery converges (with respect to effect size) to the true heterogeneity characterization.

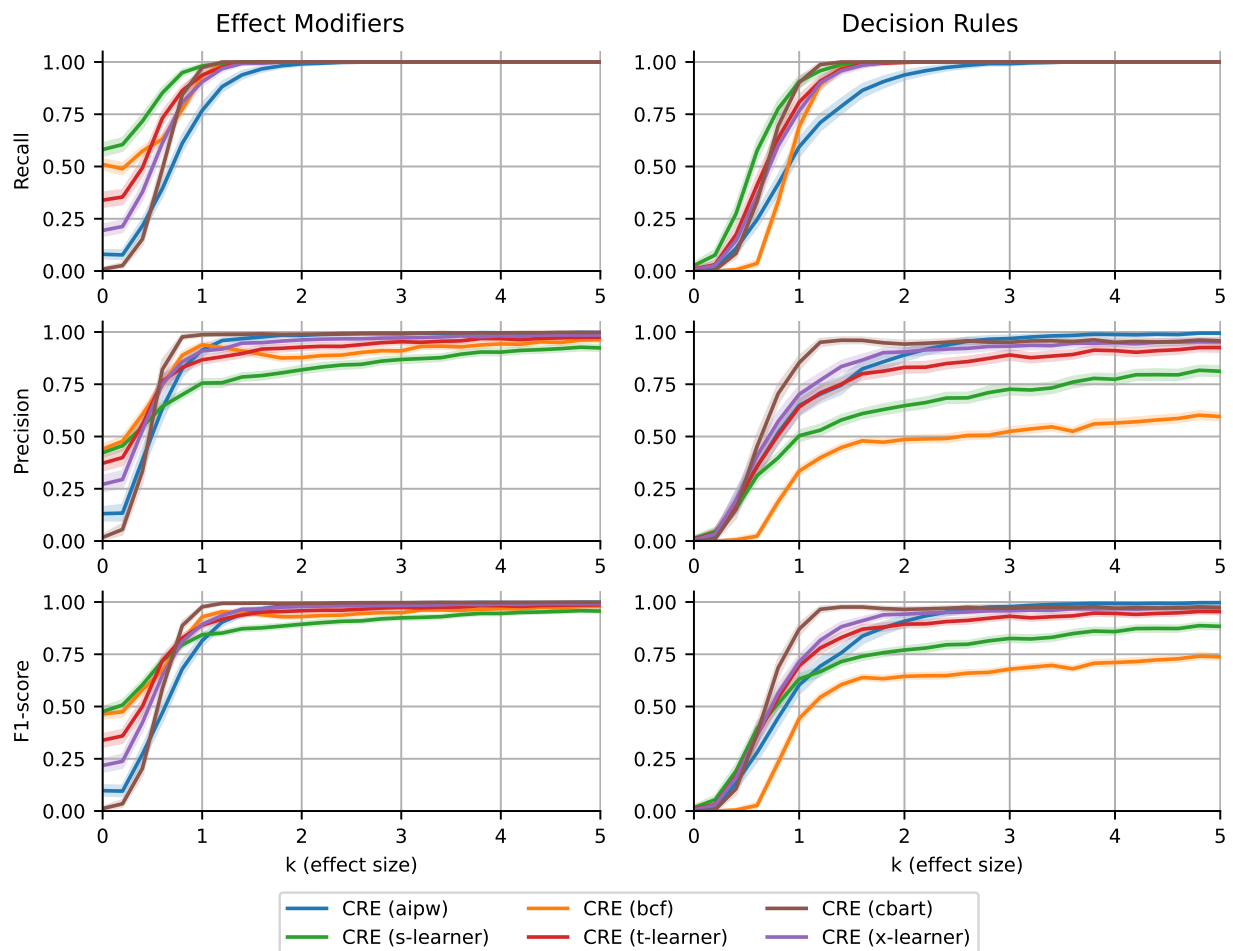


Figure D.5: Simulation study for heterogeneity discovery results with 2 rules, non-linear confounders, and 2,000 observations. Mean *Precision*, *Recall*, and *F1 – score* (lines) with the corresponding 95% confidence intervals (bands) over 250 Monte Carlo experiments are reported for each method and causal effect size k . For each CRE variant, the heterogeneity characterization converges (with respect to effect size) to the true heterogeneity characterization.

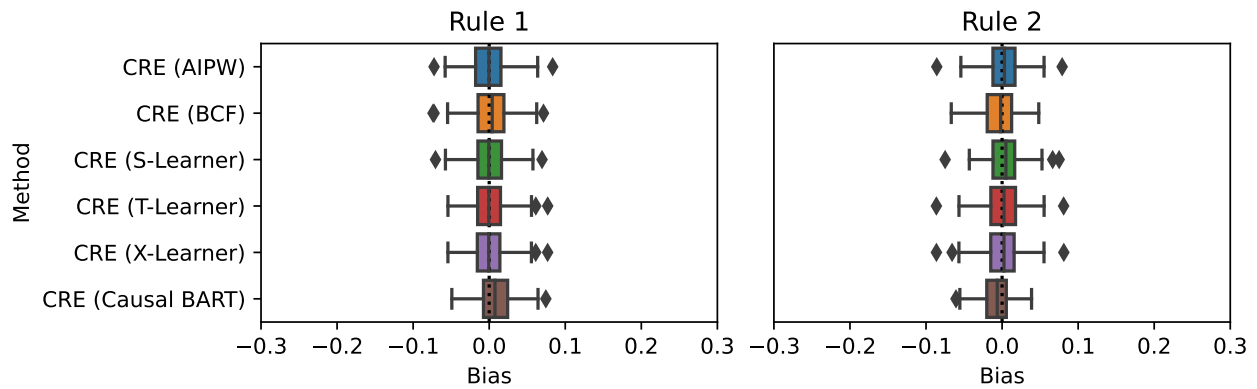


Figure D.6: Simulation study for HTE estimation, with $M = 2$ rules, linear confounding and 5,000 individuals. For all the CRE variants, for each rule, the AATE's bias over 250 Monte Carlo experiments is reported in a boxplot.

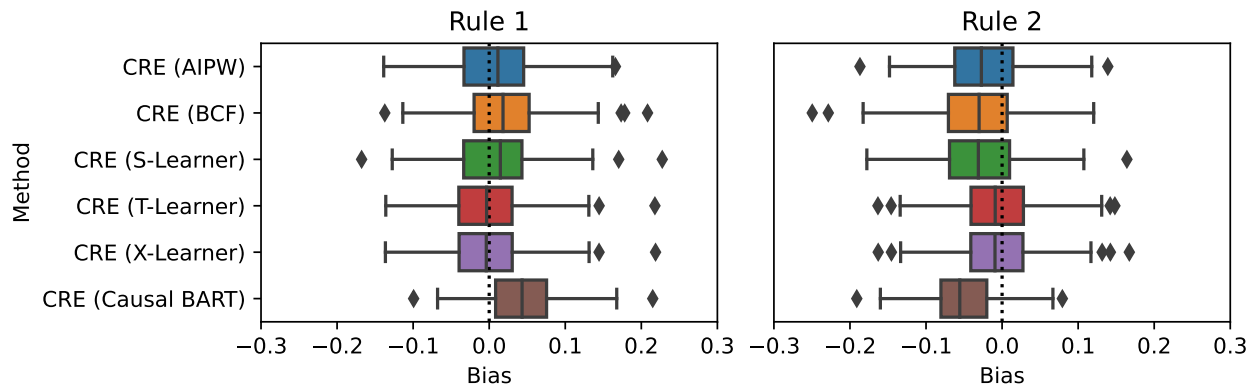


Figure D.7: Simulation study for HTE estimation, with $M = 2$ rules, linear confounding and 1,000 individuals. For all the CRE variants, for each rule, the AATE's bias over 250 Monte Carlo experiments is reported in a boxplot.

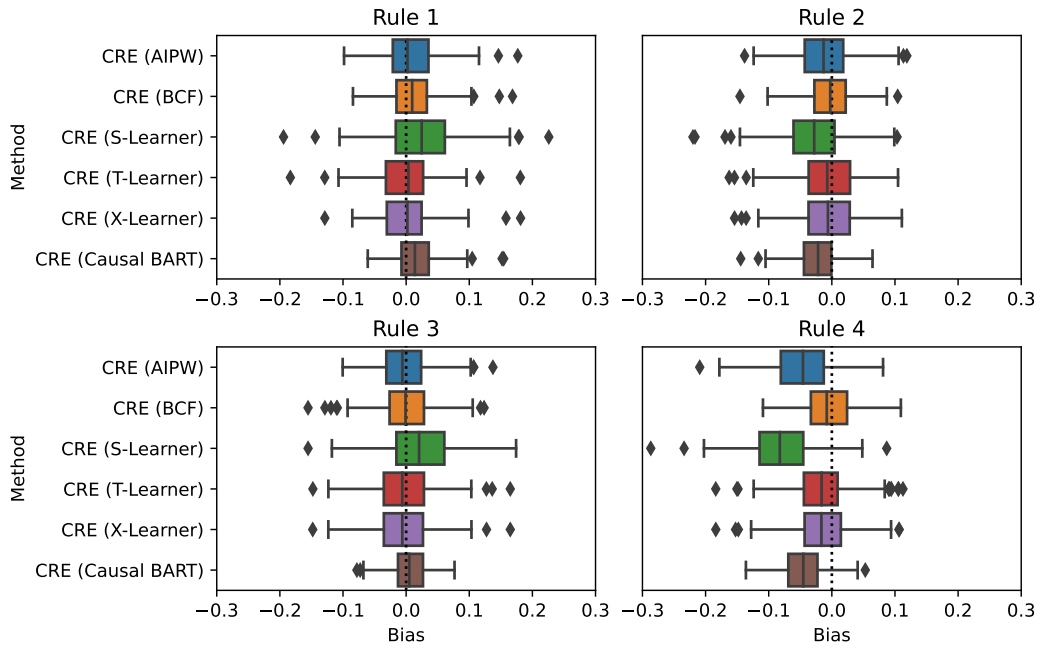


Figure D.8: Simulation study for HTE estimation, with $M = 4$ rules, linear confounding and 2,000 individuals. For all the CRE variants, for each rule, the AATE's bias over 250 Monte Carlo experiments is reported in a boxplot.

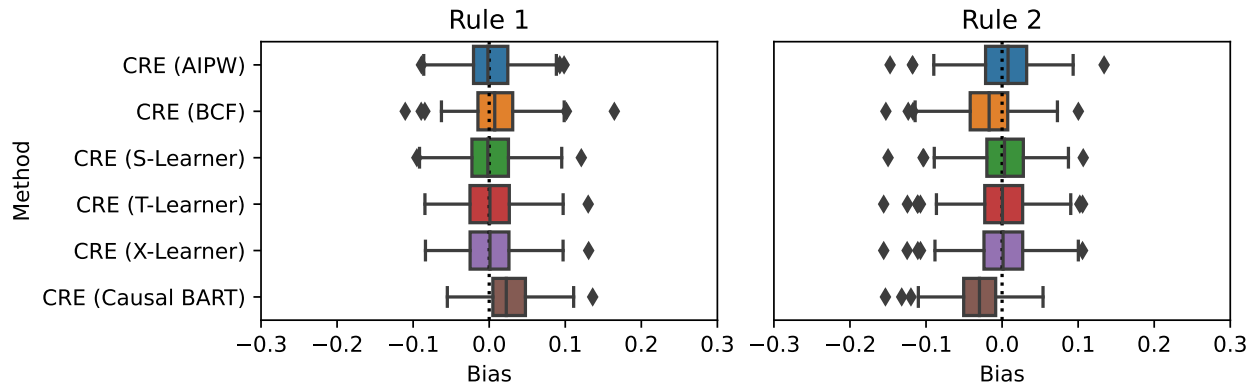


Figure D.9: Simulation study for HTE estimation, with $M = 2$ rules, no-confounding (randomized controlled trial) and 2,000 individuals. For all the CRE variants, for each rule, the AATE's bias over 250 Monte Carlo experiments is reported in a boxplot.

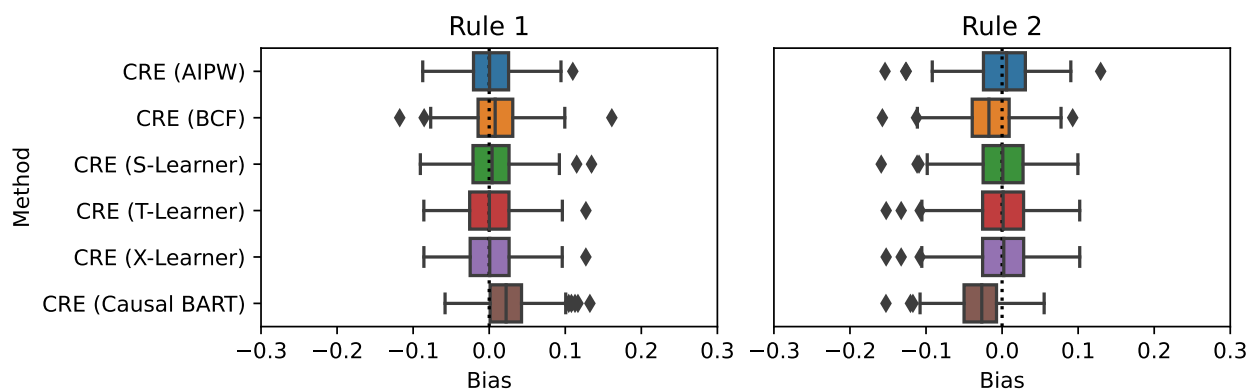


Figure D.10: Simulation study for HTE estimation, with $M = 2$ rules, non-linear confounding and 2,000 individuals. For all the CRE variants, for each rule, the AATE's bias over 250 Monte Carlo experiments is reported in a boxplot.

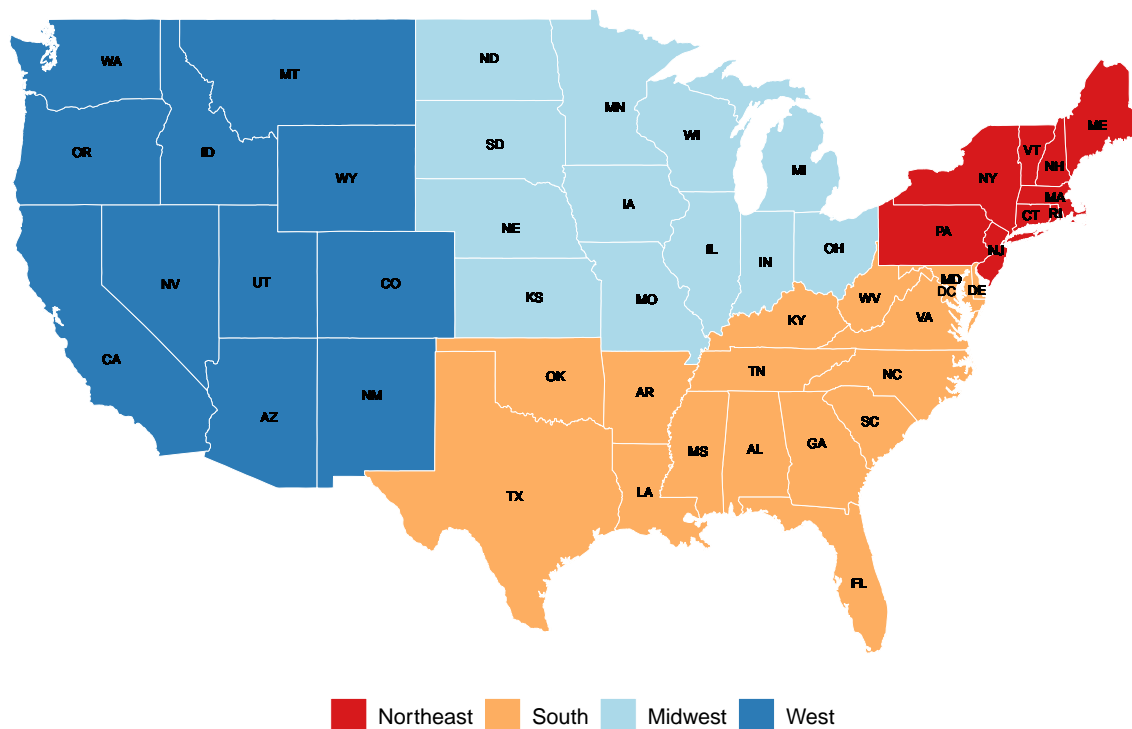


Figure F.1: Map of the four census geographical regions for the contiguous U.S.